Quaternary Science Reviews 263 (2021) 106977

Contents lists available at ScienceDirect

Quaternary Science Reviews

journal homepage: www.elsevier.com/locate/quascirev

Fluvial aggradation and incision in the Brazilian tropical semi-arid: Climate-controlled landscape evolution of the São Francisco River

Patricia Colombo Mescolotti [a, *], Fabiano do Nascimento Pupim [b], Francisco Sérgio Bernardes Ladeira [c], André Oliveira Sawakuchi [d], Amanda Santa Catharina [e], Mario Luis Assine [a]

[a] Instituto de Geociências e Ciências Exatas, Universidade Estadual Paulista - Unesp, Avenida 24A, 1515, Rio Claro, 13506-900, Brazil
[b] Departamento de Ciências Ambientais, Universidade Federal de São Paulo, Rua São Nicolau, 210, Diadema, 09913-030, São Paulo, Brazil
[c] Instituto de Geociências, Universidade Estadual de Campinas - Unicamp, R. Carlos Gomes, 250, Campinas, São Paulo, 13083-855, Brazil
[d] Instituto de Geociências, Universidade de São Paulo – USP, Rua do Lago, 562, São Paulo, 05508-080, Brazil
[e] Itt Fossil, Universidade do Vale do Rio dos Sinos – Unisinos, Avenida Unisinos, 950, São Leopoldo, Rio Grande do Sul, 93020-190, Brazil

ARTICLE INFO

Article history:
Received 25 November 2020
Received in revised form
22 April 2021
Accepted 24 April 2021
Available online 15 May 2021

Handling Editor: Xiaoping Yang

Keywords:
Late quaternary
Fluvial response
OSL dating
Fluvio-eolian interaction
Precession cycles

ABSTRACT

Large rivers are dynamic systems whose evolution depends on both internal and external forcing, particularly tectonics, sea level, and climate. Associating fluvial responses to a specific driver is a complex task that has been debated for a long time. Thus, rivers that flow exclusively under tectonically stable areas and without direct influence of relative sea level changes are suitable targets to understand how large fluvial systems responded to past climate changes. The São Francisco River is one of the largest cratonic rivers across South America, and its late Quaternary sedimentary deposits record the fluvial landscape evolution in a thousand-year timescale. The São Francisco River flows northward over different climate zones, with its upper course in a semi-humid setting, but with most of its watershed under semi-arid conditions. To understand the controls on sediment erosion, transport, and storage from uplands to lowlands, we investigated a 200-km section of the medium course of the São Francisco River in northeast Brazil. Several geomorphological zones were characterized, mapped, and dated by optically stimulated luminescence (OSL). Two zones are represented by degraded terraces with lakes, but no preserved alluvial features: (zone 1) high-level terrace (87.7 ± 12.7 ka) and (zone 2) low-level terrace (65.5 ± 5.3 to 39.3 ± 4.3 ka). Three zones comprise the active confined aggradational plain, with features such as scroll bars and abandoned channels: (zone 3) older meander belt (18.1 ± 1.6 ka); (zone 4) young meander belt (15.5 ± 1.5 to 9.5 ± 1.0 ka), and (zone 5) modern channel belt (0.4 ± 0.1 to 0.3 ± 0.1 ka). Zone 6 comprises an eolian dune field composed of parabolic dunes with two phases of active sedimentation (45.1 ± 5.2 to 25.5 ± 4.4 ka and 14.3 ± 2.6 to 5.2 ± 1.4 ka). Sediment deposition ages allowed the recognition of at least four phases of fluvial aggradation (90 ka; 66 to 39 ka; 18 to 9 ka and 0.3 ka to recent), three phases of incision (85 to 66 ka; 39 to 18 ka and 9 to 1 ka), and two phases of dune field stabilization (25 to 15 ka and 5 ka to recent). Development of the eolian dune fields occurred during drier conditions, when the inland activity of trade winds reworked sediments deposited on the fluvial plain. We interpret the incision events as having been set in motion by an increase of fluvial discharge in the upper catchment area, produced by rainfall intensification due to activity of the South Atlantic Convergence Zone (SACZ). The aggradation and incision phases on the São Francisco River during the last 100 ka are therefore likely controlled by multi-millennial precipitation changes, possibly related to precession cycles. The events of high sedimentation rate in the São Francisco river mouth are partially correlated with incision phases in its middle course. This suggests that sedimentation in plains of large plateau rivers can be decoupled from the coastal area.

1. Introduction

In tropical settings, large rivers are the main natural drivers of landscape modification, influencing the distribution of animal and

* Corresponding author.
E-mail address: pamescolotti@outlook.com (P.C. Mescolotti).

https://doi.org/10.1016/j.quascirev.2021.106977
0277-3791/

plant species (e.g., Nazareno et al., 2019; Thom et al., 2020) and the development of human societies (e.g., Singh et al., 2017). The influence of large rivers reaches beyond continental settings since their sediments and nutrients are pivotal for the maintenance of coastal and marine ecosystems (e.g., Aufdenkampe et al., 2011; Tamura et al., 2020). South America hosts six of the ten largest rivers of the world in terms of water discharge (Latrubesse et al., 2005). However, all these rivers drain wet regions in the Amazon or in southern South America. The São Francisco River is the easternmost large river of South America and it stands out as the largest river flowing over the semi-arid region of northeast Brazil.

The São Francisco River is one of the main rivers exclusively draining Brazil, with an extension of 2,900 km and a watershed with an area of 631,133 km^2, corresponding to 7.4% of the Brazilian territory (Fig. 1; Knoppers et al., 2006; Santos et al., 2012). The São Francisco River is crucial to human activities because it crosses five states from southeast to northeast Brazil, and its waters are currently being artificially re-routed to reach several other states with water supply shortages. The river has its headwaters in the transition between the Atlantic rainforest and the Cerrado biomes in the Serra da Canastra highlands, southeastern Brazil, but most of the river course drains high, dissected landscapes in the domain of tropical Caatinga dry forests. Thus, the São Francisco River also plays an important role for neotropical ecosystems in Brazil. Despite its importance to human populations and ecosystems, the long-term sedimentary dynamics of the São Francisco River and its response to climate variations have been poorly studied so far.

Geological and paleoclimatic changes in the São Francisco River drainage basin have been inferred from studies on its coastal sector and the sedimentary record of the adjacent offshore marine zone (Campos et al., 2019). An important question to understand the evolution of the São Francisco River is whether changes in the coastal region are coupled or decoupled to the entire watershed. Two factors can promote different evolutionary histories in the lower and medium river courses. Firstly, the São Francisco River flows towards north for most of its length, from headwaters located in a humid tropical region in southeast Brazil to semi-arid areas in northeast Brazil. Therefore, the river discharge in the middle and lower courses is not only influenced by local climatic conditions, but also by rainfall in the region of its springs. Secondly, the São Francisco River is a plateau river for most of its course, with local baseline levels controlled by waterfalls. Thus, the eustatic control of the erosion base level is restricted to its lowermost course.

To understand the controls on sedimentation and erosion phases in the plateau area, a 200 km stretch of the medium course of the São Francisco River in the state of Bahia was investigated (Fig. 2). This stretch is characterized by the presence of sedimentary terraces, well-developed meander belts, and the remarkable Xique-Xique eolian dune field (Oliveira et al., 1999; Barreto et al., 2002; Ab'Saber, 2006). In this work, several geomorphological zones were characterized and mapped, and the sedimentary deposits described and dated by optically stimulated luminescence (OSL). This data suite allowed us to interpret the erosive and depositional events that shaped the fluvial plain during the late Quaternary. An evolutionary outline is presented here, seeking to reconstruct the Late Pleistocene and Holocene geomorphic changes which resulted from past hydroclimate variations recorded in paleoclimate archives from the literature. The correspondence between deposition-erosion events and paleoclimate information available in the literature, as well as the comparison with studies carried out in the lower course are also discussed.

2. Geomorphological setting

The São Francisco Basin is subdivided into four geomorphological domains (Fig. 1; Pereira et al., 2007). The river has its springs in Serra da Canastra, an elevated plateau located in southeastern Brazil, with altitudes exceeding 1400 m and precipitation over 1500 mm/year, in the transition between the Atlantic Forest and the Cerrado. The upper course extends to the Pirapora city (state of Minas Gerais), before the confluence of the Das Velhas River, characterized as a river with a rocky bed that runs in an entrenched valley, with local development of a narrow alluvial plain (<2 km).

The medium course comprises a long stretch, reaching the city of Remanso (state of Bahia), with a well-developed river plain and width varying between 2 and 16 km, generally wider to the north (downstream). The stretch is in a semi-arid area, with increasing aridity to the north, where Caatinga vegetation predominates. The average precipitation decreases downstream from 1100 mm/year to 600 mm/year, concentrated between December and March, with the vegetation transitioning from Cerrado to Caatinga. The average fluvial discharge increases considerably in the beginning of this stretch, from about 800 m^3 s^{-1} in Pirapora to about 2000 m^3 s^{-1} in the city of Januária, due to contribution from the Das Velhas, Paracatu and Urucuia rivers. Its climate is influenced by the South American summer monsoon (SAMS) and by the South Atlantic Convergence Zone (SACZ) (Chaves and Cavalcanti, 2001). The winds acting in the area are seasonal, with higher intensities during the dry season (July to August), and come from southeast and east, with an average speed of 7.5 m/s (Santos et al., 2013).

The sub-medium course presents higher slopes with rapids and waterfalls, dominance of a rocky bed and subordinate development of alluvial plains. The main knickpoint is located at the Paulo Afonso waterfall, which originally was 80 m high but is now partially covered by the waters of the Paulo Afonso hydroelectric dam reservoir (Fig. 1). This portion is in the semi-arid area, where Caatinga vegetation predominates and rainfall is around 500 mm/year, concentrated between March and June.

The lower course has a rocky bed for most of its extension, with the development of a river plain in the last 70 km. Fluvial discharge varies greatly due to seasonal droughts inland, with a long-term average of around 3000 m^3 s-1. Before flowing into the Atlantic Ocean, the river crosses a series of subparallel coastal strandplains present on both banks, partially covered by Holocene eolian dunes (Dominguez et al., 1983; Barbosa and Dominguez, 2004).

The investigated area is in the middle course of the São Francisco River, in the state of Bahia, located upstream and in an area not affected by the Sobradinho hydroelectric reservoir, built in 1979 (Fig. 1). In the studied section, the fluvial plain is well developed, with the elongated fluvial sedimentation oriented approximately N40E, and the current channel predominantly on its left side (Fig. 2). The river has an average annual fluvial discharge of about 2500 m^3 s^{-1}, with only the Grande River, with its mouth in the city of Barra, as an important tributary. The area is a lowland bordered by high reliefs carved out of Proterozoic rocks; to the east by Chapada Diamantina (metasediments) and to the west by quartzites from Serra do Estreito (Northern Espinhaço), a narrow and elongated NS-oriented ridge. The local base level of the area is controlled by the Paulo Afonso waterfall (Fig. 1). The region is a dryland with semiarid climate (Bsh) according to the Köppen classification (Alvares et al., 2013), and the dominant vegetation is Caatinga (cacti, shrubs and spiny and bromeliad trees), with *Mauritia vinifera* palm swamp (*veredas*) found associated with natural drains (Oliveira et al., 1999).

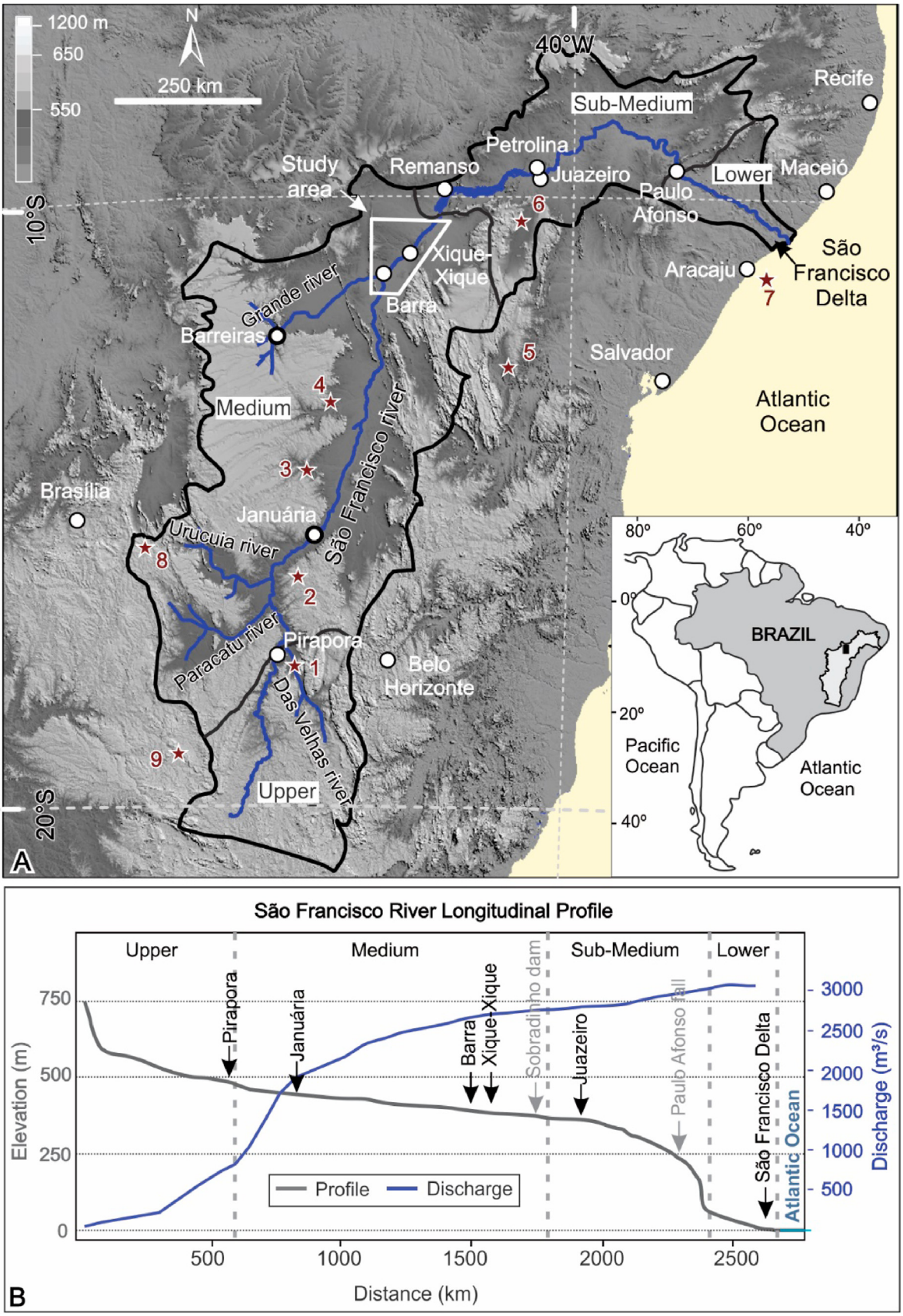

Fig. 1. A) Shuttle Radar Topography Mission products (SRTM) model (90 m) of the São Francisco River Basin and its sectors (black polygon), with location of the study area, caves, lake, and the marine core from the São Francisco river mouth (stars). Sites mentioned in the text: 1. Das Velhas River, tributary of the upper São Francisco River (Magalhães Jr. et al., 2011); 2–3. Central-eastern caves (2- Lapa Sem Fim, 3-Lapa Grande) (Strikis et al., 2015, 2018); 4. Padre cave (Wang et al., 2007); 5. Paixão and Marota caves (Strikis et al., 2015,

3. Methods

3.1. Remote sensing and geomorphological mapping

The geomorphological survey was carried out based on the definition of geomorphological zones characterized by different landscapes, and their mapping on the presence of distinct landform associations. The relative dating of zones was based on geometric criteria such as truncation of landforms by younger units, and on the topographic elevation in relation to the current river channel. For the recognition and mapping of landforms, we used images from optical sensors (Landsat 8 OLI/TIRS Level-2) and digital elevation models (DEM) from the Shuttle Radar Topography Mission products (SRTM/C-band). DEMs were elaborated based on the customization of palettes and colors with intervals ranging from 1 to 15 m, aiming to highlight geomorphological features with low topographic amplitude (Merino et al., 2015).

3.2. Sedimentary facies analysis

Sedimentary facies were described in natural outcrops in riverbanks and road cuts in shallow trenches. For some of the zones it was possible to establish the facies stacking based on survey of vertical profiles on both banks of the São Francisco River, with thicknesses ranging from 0.7 to 7.5 m. Different paleosol profiles (sensu Rettalack, 2001; Schoeneberger et al., 2012) have been described, with horizon identification, color characterization, thickness, contacts, consistency and presence or not of cementation, degree of bioturbation, and presence of pedogenetic features (e.g., nodules). Samples were collected at different levels for OSL dating. Chemical analyzes for routine pedology and grain size analyses were performed only on samples of soil profiles that are more representative of the units described. The analyzes included pH determination, exchangeable aluminum ($Al+^{3}$), saturation by exchangeable aluminum, sodium, calcium, magnesium and potassium ($Na+$, $Ca+^{2}$, $Mg+^{2}$, $K+$), organic matter, sum of bases (SB), base saturation (V value), total cation exchange capacity (T), and resin phosphorus (P-res), following the procedures from Camargo et al. (2009).

3.3. OSL dating

OSL dating was performed on quartz sand grains at the Luminescence and Gamma Spectrometry Laboratory (LEGaL), Institute of Geosciences of the University of São Paulo (IGc-USP). Sediment samples were collected and dated by OSL, yielding 15 ages of alluvial deposits and 10 of eolian sediments (Tables 1 and 2). Sample preparation for equivalent dose (D_e) measurements followed standard procedures (Aitken, 1985). Samples were wet-sieved to isolate the 180–250 μm grain-size fraction. The target fraction was treated with hydrogen peroxide (H_2O_2, 27%) and hydrochloric acid (HCl, 10%) to remove organic matter and carbonate minerals, respectively. Heavy mineral (>2.75 g/cm^3) and feldspar (<2.62 g/cm^3) grains were removed by heavy liquid separation with a lithium metatungstate solution. Then, quartz concentrates (2.62 and 2.75 g/cm^3) were etched with hydrofluoric acid (HF, 38%) for 40 min to remove remnant feldspar grains and etch the ~10 μm of the outer layer of quartz grains, thus removing the alpha particles' contribution from the radiation dose rate.

Aliquots of quartz grains (100 and 200 grains) were mounted on aluminum discs for luminescence measurements on two automated Risø TL/OSL DA-20 reader systems equipped with $^{90}Sr/^{90}Y$ beta sources that delivered dose rates of 0.075 ± 0.001 and 0.109 ± 0.001 Gy/s, blue LEDs (470 ± 20 nm) operated at 90% power (~40 mW/cm^2) for stimulation and Hoya U-340 filter for light detection in the ultraviolet band (290 and 340 nm) with a bialkali PM tube (Thorn EMI 9635QB). The single-aliquot regenerative dose (SAR) protocol (Murray and Wintle, 2000, 2003) was used to estimate the equivalent dose (D_e) (Table S1- supplementary material). OSL signal was calculated using the initial 0.8 s integral of light emission with subtraction of the normalized last 10 s of light emission as background. Only aliquots with recycling ratio values between 0.90 and 1.10, recuperation less than 5% and negligible IR signal were used in the equivalent dose calculations. Equivalent doses for age calculation of each sample were calculated through the Central Age Model (Galbraith et al., 1999).

Dose recovery tests were performed on eolian and fluvial samples, with 4 aliquots per test, with given doses of 5 and 15 Gy for eolian samples and 5, 10 and 50 Gy for fluvial samples. Preheat temperatures of 200 °C, 240 °C and 260 °C were tested using the SAR protocol (Murray and Wintle, 2003). The best dose recovery results for eolian samples were obtained for a preheat of 240 °C. Calculated-to-given dose ratios using this preheat temperature were 1.00 ± 0.02 for a given dose of 5 Gy and 0.99 ± 0.02 for a given dose of 15 Gy. The best dose recovery results for fluvial samples were obtained with a preheat of 260 °C. Calculated-to-given dose ratios were 1.03 ± 0.02, 0.94 ± 0.02 and 0.98 ± 0.03, respectively for given doses of 5, 10 and 50 Gy. Additional information on the dose recovery tests can be found in the supplementary materials (Table S2).

For radiation dose-rate calculation, natural radionuclides concentrations were measured through high-resolution gamma-ray spectrometry in a high-purity germanium detector (HPGe; relative efficiency of 55%; 2.1 keV energy resolution) encased in an ultralow background shield (Canberra Industries). U, Th and K concentrations were converted to dose rates using factors proposed by Guerin et al. (2011). Water saturation was determined by the ratio between water weight and dry sample weight [(water weight/dry sample weight) x100]. We used a relatively high water saturation uncertainty of ±10% error to cover possible variation in water content through time. The cosmic dose rate contribution was calculated using sample depth, elevation, latitude, and longitude, as described by Prescott and Hutton (1994).

4. Results

4.1. OSL chronology

Quartz grains with high luminescence sensitivity predominate in the dated sediments, with dose-response curves well described by a single saturating exponential function (Figure S1 - supplementary material). The equivalent doses calculated for the 25 samples ranged from 0.3 ± 0.1 to 62.8 ± 3.2 Gy, and the total dose rate ranged from 0.3 ± 0.1 to 1.4 ± 0.1 Gy/ka (Table 1). The fluvial samples showed equivalent dose distributions with relatively low to moderate overdispersion values (13–36%; Figure S1 - supplementary material), ensuring the use of the Central Age Model. According to Arnold and Roberts (2009), well-bleached sediments without significant post-depositional mixing can present equivalent dose distributions with overdispersion of up to 35%. The only exception is the fluvial sample P13, which showed overdispersion of 93%. Thus, its age should be considered with caution, despite its consistency with the stratigraphy based on ages with lower overdispersion.

2018); 6. Caves and travertine deposits of Northeast Brazil (Wang et al., 2004); 7. Core M125-9503 (Campos et al., 2019); 8. Lagoa Feia in central Cerrado (Cassino et al., 2020); 9. Lagoa Campestre in Salitre (Ledru et al., 1996). B) Profile and mean discharge of the São Francisco River (ANA, 2014), with delimitation of sectors of the São Francisco basin.

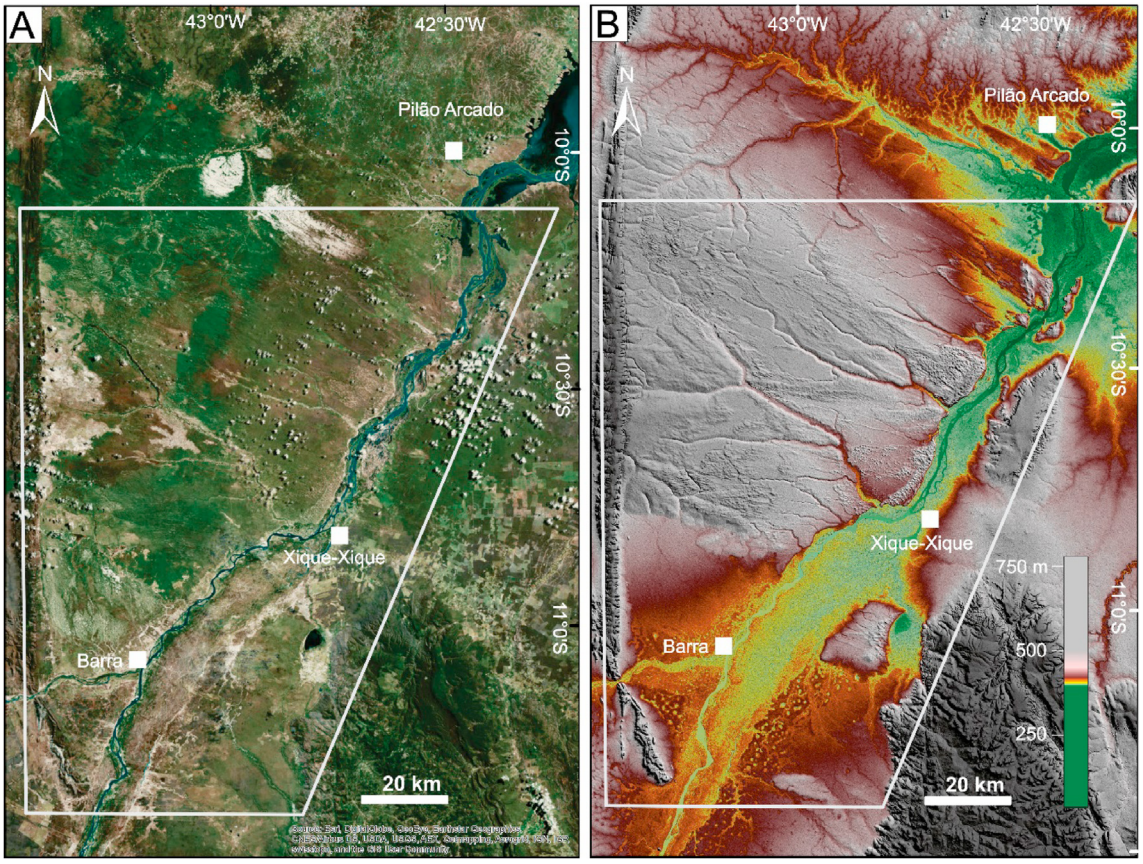

Fig. 2. Study area (white polygon). A) Aerial image extracted from the World Imagery plugin from ArcGIS online; B) DEM - SRTM (30 m).

Four eolian samples showed equivalent dose distributions with relatively high overdispersion, with values ranging from 42% to 67%. Assuming that eolian sediments experience complete bleaching prior to deposition, the high overdispersion values are likely associated to post-depositional mixing by bioturbation or beta-dose heterogeneities. Sediments with low dose rate such as our studied eolian samples are more likely to be affected by beta dose rate heterogeneities due to the presence of hotspots of radionuclides concentration (Smedley et al., 2020). Despite five samples having equivalent dose distributions with high overdispersion, most studied samples are considered well-bleached sediments without evidence of significant post-depositional mixing or dose rate heterogeneities affecting equivalent dose distributions. The studied deposits show sediment deposition ages ranging from 87.7 ± 12.7 to 0.3 ± 0.1 ka, can be considered accurate. These ages (Tables 1 and 2) were used to constrain phases of sediment accumulation and erosion recorded in the geomorphological zones described in the next sections.

4.2. Geomorphological zones and sedimentary facies

Seven distinct geomorphological zones were recognized and defined in the study area (Fig. 3 and Table 2). Two zones are older degraded surfaces, topographically higher and forming terraces made up of older alluvial deposits. They are surfaces with low relief variations and gentle declivity roughly following the current gradient of the river, towards NNE (Fig. 4). Three zones comprise the aggradational plain of the São Francisco River, confined to an incised valley limited by the hillslope of the marginal terraces. Two abandoned amalgamated meander belts (older and young) with preserved original river morphologies function as the floodplain of the modern channel belt. Eolian dune fields make up another zone of active sedimentation. A set of coalescent alluvial fans present in the southern part of the left riverbank (but not described here) constitutes the seventh recognized morphological zone. The channels that form the fans are ephemeral and rework the sands of the dunes located to the north. The fans have a typical distributive drainage pattern and advance over the surface of the oldest terraces.

The six compartments analyzed were validated in the field, with observation of their depositional forms and description of sedimentary facies (Table 2). As this is an area with low topographic relief, outcrops are scarce, making it difficult to recognize facies architecture elements. Exposures occur mainly on the erosive banks of the current river channel, especially on its left bank. Some less expressive vertical exposures were found in the small tributary channels present in some zones, complemented by the opening of shallow trenches.

4.2.1. High-level terrace

The high-level terrace (HLT) is a degradational surface that has no genetic relationship to the aggradational plains related to the evolution of the current river, as its area is much wider and extends towards east and west, reaching the foothills of the uplands that limit the lowlands of the São Francisco Basin (Fig. 3). This surface is a low-relief landscape with altimetric variations ranging from 405 to 415 m, slightly tilted to the northeast in the downstream direction (Fig. 4). Elevated 10–20 m above the river, this morphological zone is not reached by the waters of the São Francisco River during floods.

Table 1
Equivalent doses in quartz grains, radiation dose rates and OSL ages from the São Francisco River, Bahia, Brazil. *Sample P10 has potassium concentration below detection limit (0.001%), which was considered for dose rate calculation.

Zones	Sample ID	Lab code	Depth (m)	U (ppm)	Th (ppm)	K (%)	Cosmic dose rate (Gy/ka)	Water sat. (%)	Total dose rate (Gy/ka)	Equivalent Dose (Gy)	N	OD (%)	OSL age (ka)
HLT	P04	L1030	1.1	0.55 ± 0.02	2.86 ± 0.11	0.138 ± 0.007	0.18 ± 0.08	0.21 ± 10	0.65 ± 0.09	57.1 ± 2.2	32	21	**87.7 ± 12.7**
LLT	P01 D	L1029	3.8	0.52 ± 0.02	2.09 ± 0.06	0.217 ± 0.008	0.12 ± 0.01	0.78 ± 10	0.62 ± 0.04	36.1 ± 1.6	17	18	**58.6 ± 4.9**
	P02 C	L1287	2.7	1.03 ± 0.04	6.80 ± 0.24	0.311 ± 0.014	0.18 ± 0.09	0.71 ± 10	1.22 ± 0.13	47.8 ± 1.5	22	14	**39.3 ± 4.3**
	P02 D	L1286	3.2	1.11 ± 0.05	8.24 ± 0.28	0.405 ± 0.018	0.16 ± 0.05	0.87 ± 10	1.42 ± 0.12	62.8 ± 3.2	18	21	**44.4 ± 4.3**
	P02 E	L1284	5.2	0.75 ± 0.03	3.60 ± 0.14	0.173 ± 0.009	0.16 ± 0.02	0.74 ± 10	0.77 ± 0.06	32.2 ± 1.0	22	13	**41.6 ± 3.4**
	P05	L1283	7	0.41 ± 0.02	1.36 ± 0.07	0.192 ± 0.009	0.12 ± 0.01	0.11 ± 10	0.51 ± 0.04	33.6 ± 1.2	22	16	**65.5 ± 5.3**
OMB	P06 A	L1019	1.2	0.69 ± 0.02	3.07 ± 0.08	0.338 ± 0.011	0.17 ± 0.03	0.51 ± 10	0.88 ± 0.07	16.3 ± 0.7	22	19	**18.1 ± 1.6**
YMB	P14	L1292	1.2	1.17 ± 0.05	2.08 ± 0.10	0.033 ± 0.004	0.17 ± 0.03	0.23 ± 10	0.60 ± 0.05	6.1 ± 0.3	22	20	**9.6 ± 0.9**
	P13	L1297	0.7	0.31 ± 0.02	0.84 ± 0.05	0.013 ± 0.003	0.19 ± 0.05	0.22 ± 10	0.32 ± 0.06	5.0 ± 1.2	40	93	**15.0 ± 4.4**
	P12	L1296	1.6	0.48 ± 0.02	1.02 ± 0.06	0.009 ± 0.003	0.17 ± 0.02	4.94 ± 10	0.35 ± 0.03	5.5 ± 0.3	22	28	**15.5 ± 1.5**
	P02 A	L1289	0.7	0.61 ± 0.03	1.94 ± 0.09	0.100 ± 0.006	0.18 ± 0.05	0.04 ± 10	0.54 ± 0.06	5.4 ± 0.2	24	21	**9.5 ± 1.0**
	P02 B	L1288	1	0.72 ± 0.03	3.31 ± 0.13	0.193 ± 0.009	0.18 ± 0.08	0.21 ± 10	0.73 ± 0.09	7.9 ± 0.6	23	36	**10.1 ± 1.5**
MCB	P10	L1478	0.9	3.28 ± 0.10	10.51 ± 0.46	<0.001 ± 0.001	0.18 ± 0.06	11.31 ± 10	1.53 ± 0.12	0.4 ± 0.1	18	14	**0.3 ± 0.1**
	P09 A	L1023	3.6	0.63 ± 0.02	3.15 ± 0.08	0.310 ± 0.010	0.13 ± 0.01	0.70 ± 10	0.77 ± 0.06	0.3 ± 0.1	12	17	**0.4 ± 0.1**
	P09 B	L1022	4.7	0.46 ± 0.02	1.76 ± 0.06	0.392 ± 0.012	0.11 ± 0.01	0.43 ± 10	0.71 ± 0.05	0.3 ± 0.1	9	31	**0.4 ± 0.1**
EDF	P11	L1369	0.6	0.24 ± 0.02	0.55 ± 0.04	0.001 ± 0.001	0.19 ± 0.06	0.47 ± 10	0.29 ± 0.06	1.5 ± 0.2	13	42	**5.2 ± 1.4**
	P15	L1402	0.5	0.37 ± 0.02	1.16 ± 0.07	0.076 ± 0.006	0.18 ± 0.07	0.03 ± 10	0.43 ± 0.08	3.3 ± 0.5	22	64	**7.5 ± 1.8**
	P18 B	L1403	1.5	0.43 ± 0.02	1.42 ± 0.08	0.021 ± 0.003	0.17 ± 0.02	0.04 ± 10	0.39 ± 0.03	3.0 ± 0.1	19	16	**7.6 ± 0.7**
	P20	L1295	1.6	0.22 ± 0.02	0.66 ± 0.05	0.154 ± 0.008	0.17 ± 0.02	0.03 ± 10	0.42 ± 0.03	5.8 ± 0.2	22	13	**13.7 ± 1.2**
	P06 B	L1018	0.4	0.38 ± 0.01	1.49 ± 0.05	0.282 ± 0.009	0.19 ± 0.09	0.24 ± 10	0.68 ± 0.11	9.7 ± 0.9	23	46	**14.3 ± 2.6**
	P19	L1293	1.6	0.27 ± 0.02	1.24 ± 0.07	0.019 ± 0.003	0.17 ± 0.02	0.05 ± 10	0.34 ± 0.03	8.6 ± 1.3	20	67	**25.5 ± 4.4**
	P01 A	L1278	0.3	0.33 ± 0.02	1.07 ± 0.06	0.077 ± 0.005	0.20 ± 0.13	0.02 ± 10	0.42 ± 0.13	4.9 ± 0.4	21	34	**11.5 ± 3.7**
	P01 B	L1279	2.9	0.31 ± 0.02	0.91 ± 0.06	0.077 ± 0.005	0.14 ± 0.01	0.03 ± 10	0.36 ± 0.02	13.0 ± 1.2	10	28	**36.2 ± 4.1**
	P01 C	L1014	3.1	0.21 ± 0.01	0.63 ± 0.03	0.052 ± 0.003	0.15 ± 0.02	0.03 ± 10	0.30 ± 0.02	12.3 ± 0.6	17	19	**41.4 ± 3.6**
	P21	L1372	1.4	1.14 ± 0.05	5.64 ± 0.20	0.324 ± 0.015	0.18 ± 0.03	0.26 ± 10	1.18 ± 0.09	53.2 ± 4.5	18	31	**45.1 ± 5.2**

The degradation of the surface is uneven, with dissection higher on the western side of the river (Fig. 5). Erosive processes result from the rainwater runoff and ephemeral channels from the adjacent uplands, which form an incipient tributary network and drain the waters into the São Francisco river plain. This superimposed drainage network is formed by intermittent streams, whose erosion base level is the current river channel.

Alluvial depositional forms do not exist on the surface of the unit, which is characterized by the presence of depressed, circular, and semi-circular features that form lakes with variable dimensions, from tens of meters to 1.2 km in diameter (Fig. 6). Most of the lakes are ephemeral, drying out completely during prolonged periods of drought, common in this semi-arid region of Northeast Brazil.

The deposits are dominantly composed of medium to very coarse gray sands (Fig. 7). Thin levels of gravel, with sub-rounded clasts and sandy matrix, occur interspersed with the sands. Sedimentary structures are commonly obliterated by pedogenesis, but it is possible to recognize cross-stratification in some layers. Only one sample recovered from the upper part of the terrace at the point P04 was dated, with an OSL age of 87.7 ± 12.7 ka (Table 1).

The sediments are locally cemented by silica, forming sandstones and clast-supported conglomerates (Point P03). Pedogenesis is common, with many horizons with strong gleization, intense bioturbation, mottling and clay skins. Paleosols can reach thicknesses of up to 3 m and the horizons do not have defined limits, with characteristic $CaCO_3$ cementation in the basal horizons. The tops of the soils are truncated, probably eliminated by erosion on the degrading surface.

4.2.2. Low-level terrace

The low-level terrace (LLT) has no preserved depositional shapes. It is present on almost all of the right bank of the São Francisco River and occurs as restricted and discontinuous deposits on the left bank (Fig. 3), forming elevated surfaces on both sides of the NE-oriented valley of the aggradational river plains. It occurs 4–6 m below the hillslope of the oldest surface (HLT), (Figs. 4 and 5). Its surface also has circular non-perennial lakes; however, they are smaller (diameter <100 m) and in significantly smaller quantity than on the HLT (Fig. 6).

This unit is formed by layers of fine/very fine white sand with silty-clayey intervals, sometimes constituting sequences of facies with fining upwards stacking pattern. Sedimentary structures such as cross-stratification are present in the sands but are commonly poorly preserved and/or obliterated by pedogenetic features. Typical deposits of this unit occur at the lower part of the P02 vertical profile, characterized by interleaved layers of sands and fine-grained sediments, with intense $CaCO_3$ cementation that increases towards the top (Fig. 7). Five OSL ages, between 65.5 ± 5.3 and 39.3 ± 4.3 ka (Table 1), indicate that the deposits preserved on this terrace were deposited during the Late Pleistocene.

The deposits show evidence of intense pedogenesis, with significant textural variations. The paleosols have Bt (with clay skins) and Bk (with carbonate nodules, hardened and highly reactive to HCl) horizons. Root marks are common, and the Bt horizons have well-developed prisms and blocks. In most exposures, the upper part of the profile is calcified, with $CaCO_3$ rhizolites. Locally, the calcification was so intense that no original features of the deposit or pedological structures are observed, as is the case in the riverbank in the city of Xique-Xique (P17). Chemical data shows quite high bases saturation at the base of the pedogenetic profiles and correlation of Ca and Mg with carbonate horizons and/or with rhizoconcretions (Fig. 8).

4.2.3. Older meander belt

The older meander belt (OMB) records an older river plain, with an average altimetric difference of approximately 4 m in relation to the LLT. This paleo-meander belt is more developed in the southern part of the area, where the river plain is wider (Fig. 3). As it is only 1–3 m topographically higher than the current river, a large part of this morphological zone is flooded during periods of river flooding, with the superficial flow of runoff towards north of the area, following the terrain gradient towards the river.

Scroll bars predominate over the entire length of this paleo-

Table 2
Geomorphological Zones, sedimentary features and OSL ages of the São Francisco River, Bahia, Brazil.

Gomorphological Zones		Morphology	Sedimentology	Pedological processes and features	Ages (ka)
Degradational surfaces	High-level terrace (HLT)	Low-relief landscape, with lakes from tens of meters to 1.2 km in diameter	Medium to very coarse gray sands. Thin levels of gravel, with sub-rounded clasts and sandy matrix, occur interspersed with the sands. Cross-stratification observed in some layers.	Intense gleization, abundant bioturbation, mottling and clay skins. $CaCO_3$ cementation in the basal horizons.	87.7 ± 12.7
	Low-level terrace (LLT)	Circular non-perennial lakes (diameter <100 m) less frequent than on the upper terrace	Fine/very fine white sand with silty-clayey intervals, sometimes in sequences with a fining upwards stacking pattern. Cross-stratification rarely present in the sands and/or obliterated by pedogenetic features.	Intense pedogenesis, with gradient textural. Clay skins, carbonate nodules and root marks and CaCO3 rhizolites. The upper part of the profile is calcified.	39.3 ± 4.3 41.6 ± 3.4 44.4 ± 4.3 58.6 ± 4.9 65.5 ± 5.3
Aggradational fluvial plains	Older meander belt (OMB)	Large number of paleochannels and scroll bars; flooded during periods of river flooding	Sand layers 1–2 m thick, sometimes with cross-stratification, interspersed with layers of silty-clayey sediments.	The soils are clayey, waxy and with mottled horizons, with a well-developed pedogenesis; bioturbation poorly developed.	18.1 ± 1.6
	Young meander belt (YMB)	Scroll bars are the dominant depositional feature, highlighted by arboreal vegetation in the scroll ridges.	Predominance of fine-grained deposits, with some layers of fine-grained sand	The soils are clayey, with waxy and mottled horizons. Coexistence of manganese films and iron nodules with carbonate nodules indicate polygenesis conditions.	9.5 ± 1.0 9.6 ± 0.9 10.1 ± 1.5 15.0 ± 4.4 15.5 ± 1.5
	Modern channel belt (MCB)	The channel is 300–900 m wide and has low sinuosity (~1.1), with active lateral and central sand bars.	Decimetric sets of medium to coarse-grained sands with cross-stratification and fine sands with climbing ripples, in fining-upward sequences interspersed with layers of silty-clayey sediments	Incipient pedogenesis, with bioturbation and Fe and Mn mottling, mainly in clay deposits	0.3 ± 0.1 0.4 ± 0.1 0.4 ± 0.1
Eolian dune field (EDF)		Sand sheets and parabolic dunes (simple and compound dunes), with trailing arm length varying between 0.3 and 16.3 km	Well-sorted fine/medium-grained quartz sands; cross-stratification and concentrations of millimeter-sized charcoal fragments sometimes observed	Incipient pedogenesis with root bioturbations and no pedogenesis	5.2 ± 1.4 7.5 ± 1.8 7.6 ± 0.7 11.5 ± 3.7 13.7 ± 1.2 14.3 ± 2.6 25.5 ± 4.4 36.2 ± 4.1 41.4 ± 3.6 45.1 ± 5.2

meander belt. Shapes of abandoned channels preserved on its surface are 100–300 m wide, smaller than the current channel. They show bifurcations and rejoin features suggesting that the river presented an anabranching pattern before abandonment. Many of them work as conduits during floods, draining the waters to the northeast towards the river. Small ephemeral tributary channels, which exist on the surface truncating the scrolls, also function as drainage channels after the floods (Fig. 6).

Exposures of deposits from this unit are scarce and thin, dominantly of sand layers 1–2 m thick, sometimes with cross-stratification, interspersed with layers of silty-clayey sediments. Sedimentary structures are often obliterated by pedogenesis, which affects both sandy and silty-clayey levels (Fig. 9). The soils have variegated colors and are clayey, waxy and with mottled horizons. The structures are always medium to large and well developed, indicating a well-developed pedogenesis. When present, the A horizons are quite sandy, constituting Planosols. Bioturbation is poorly developed due to prevailing hydromorphic conditions.

An OSL age of 18.1 ± 1.6 ka was obtained from a sample recovered in the point P06, about 1 m below the contact with superimposed eolian deposits with an age of 14.3 ± 2.6 ka (Fig. 9; Table 1). This single age allows only the establishment of the minimum age for the OMB since the unit's deepest deposits have not been dated.

4.2.4. Young meander belt

The young meander belt (YMB) is also an abandoned meander belt, continuous and bordering the current channel throughout the investigated area. Scroll bars are the dominant depositional feature in this morphological zone, better preserved than those of OMB and highlighted by arboreal vegetation that develops in the scroll ridges. Abandoned channels preserved in the convex parts of the scrolls show that the river channels were 100–300 m wide, similar to those of the OMB.

Although in parts of the area the meander scrolls are topographically higher than those of the OMB (Fig. 5), contact relationships clearly show that the OMB tributary channels are cut by younger YMB scrolls, breaking the connection that these channels previously had with the river (Fig. 6). In addition, there is also no superposition of small tributary channels in the YMB like those existing in the OMB. Five OSL ages ranging from 15.5 ± 1.5 to 9.5 ± 1.0 ka (Table 1) indicate younger ages for this belt, suggesting continuous sedimentation from the Late Pleistocene to the Early Holocene.

In the few exposures of this unit, channel sands can be seen truncating fine-grained deposits from the unit itself or in diastema over deposits from older units (Fig. 7). As with OMB, hydromorphic conditions dominate most of the time. The soils in this unit are also commonly clayey, with waxy and mottled horizons. In some places, the coexistence of manganese films and iron nodules with carbonate nodules was observed, indicating polygenesis conditions. Horizons A are quite sandy, constituting Planosols.

The sediments of this unit overlap unconformably the older LLT deposits (P02). This depositional hiatus is confirmed by the OSL dating of samples from the two units (20 ka hiatus) and corroborated by chemical data (Fig. 8). Chronocorrelated deposits present on the Icatu River, one of the main tributaries of the São Francisco River on its left bank in the area, comprise gray-colored sands and clays.

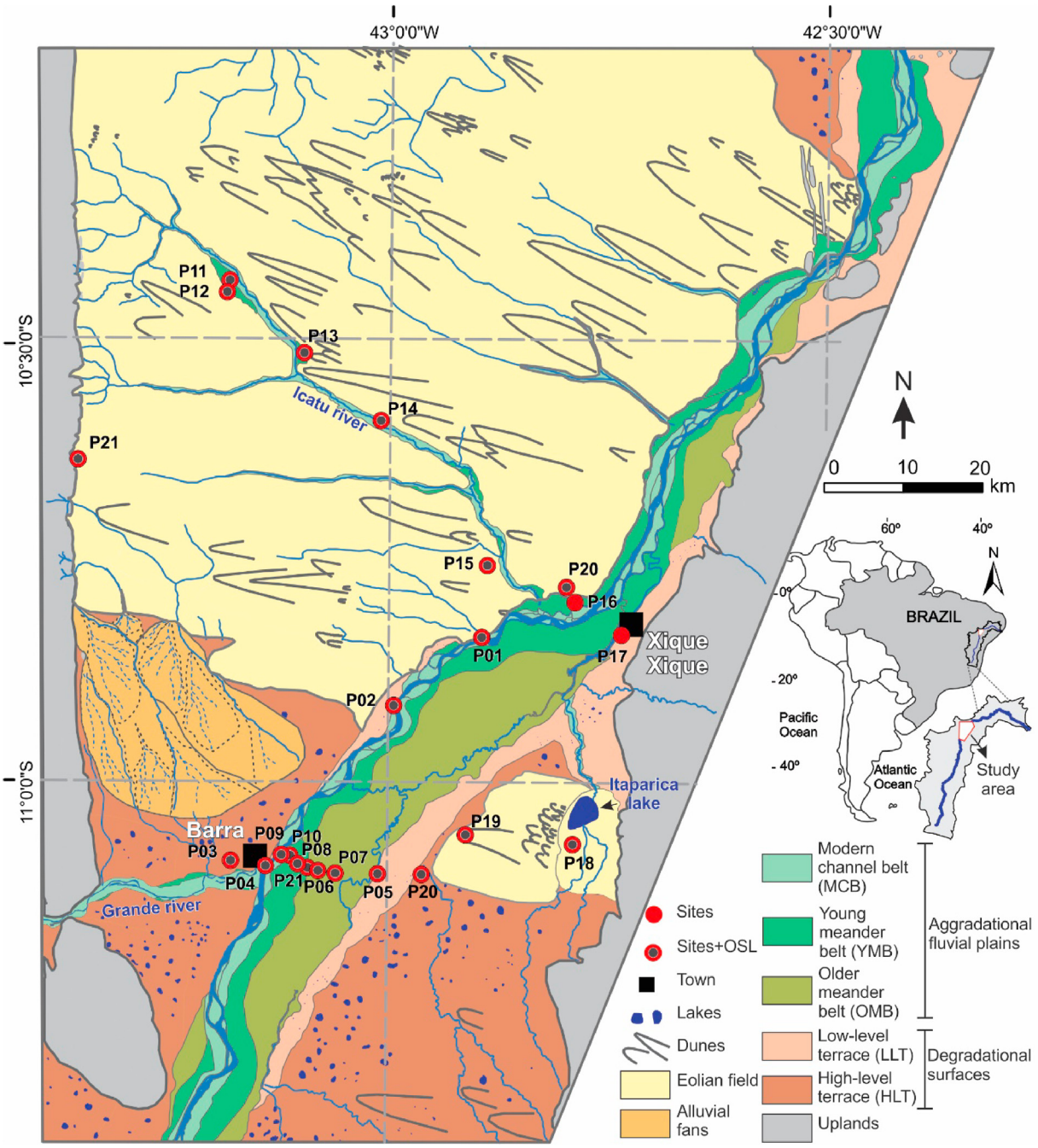

Fig. 3. Geomorphological map of the area, with location of studied sites.

4.2.5. Modern channel belt

The modern channel belt (MCB) of the São Francisco River is narrow (0.5–2.5 km) and slightly entrenched in the YMB (Fig. 3). The channel is 300–900 m wide and has low sinuosity (~1.1), with active lateral and central sand bars. The river flows in the area in three different reaches, characterized by different topographic gradients: R1 (~0.04 m/km), R2 (~0.15 m/km) and R3 (~0.02 m/km) (Fig. 4). In the upstream reach (R1), the OMB is wide and the river flows on the left bank of the river valley, often forming erosive margins on the hillslope of the terraces, with a low slope of ~0.04 m/km.

The river deflects to the east at the town of Ibiraba, 15 km west of the city of Xique-Xique, and enters the intermediate reach (R2) where the declivity increases to ~ 0.14 m/km. In this steeper reach, the river valley is confined between high ground on the right bank, where crystalline Proterozoic rocks are exposed, and the Xique-Xique dune field on the left bank (Fig. 3).

From the start of the intermediate reach, the river begins to flow within the YMB domain, with flood plains on both banks. The channel presents frequent bifurcations and rejoins, commonly with the existence of two channels with stable islands. In the downstream reach (R3) the slope decreases to ~0.02 m/km and the river presents a tendency to anabranch, with reoccupation of abandoned YMB channels. The channel belt becomes wider at this distal reach, where OCB scroll bars are not preserved.

Sedimentary deposits described show decimetric sets of

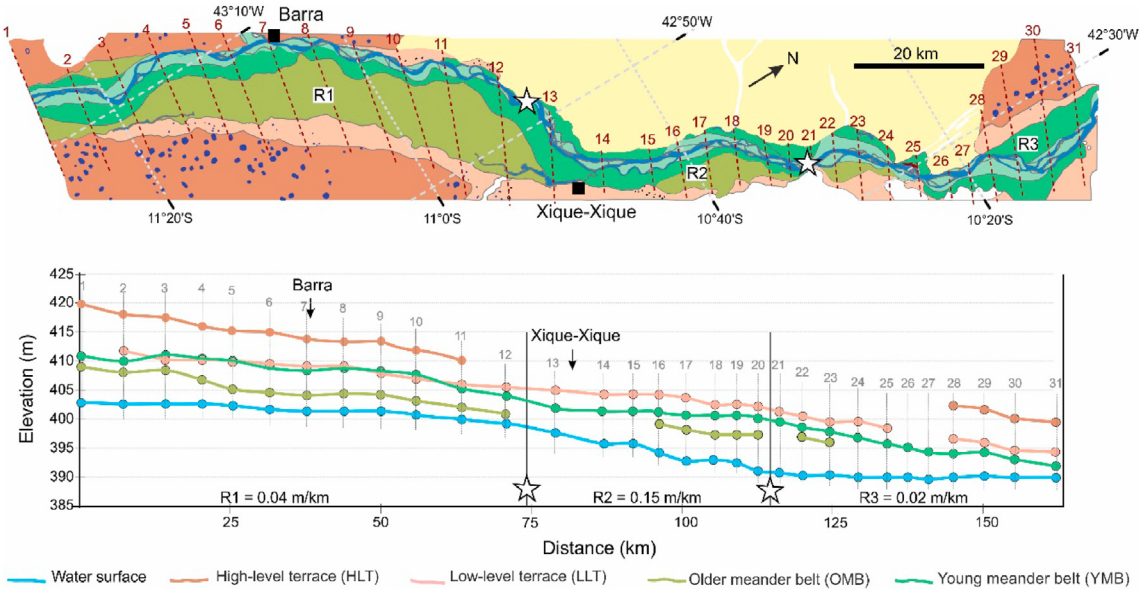

Fig. 4. Comparison of the altimetric profiles from the aggradation and degradation zones associated to the São Francisco River (R = reach). (Legend is the same as in Fig. 3).

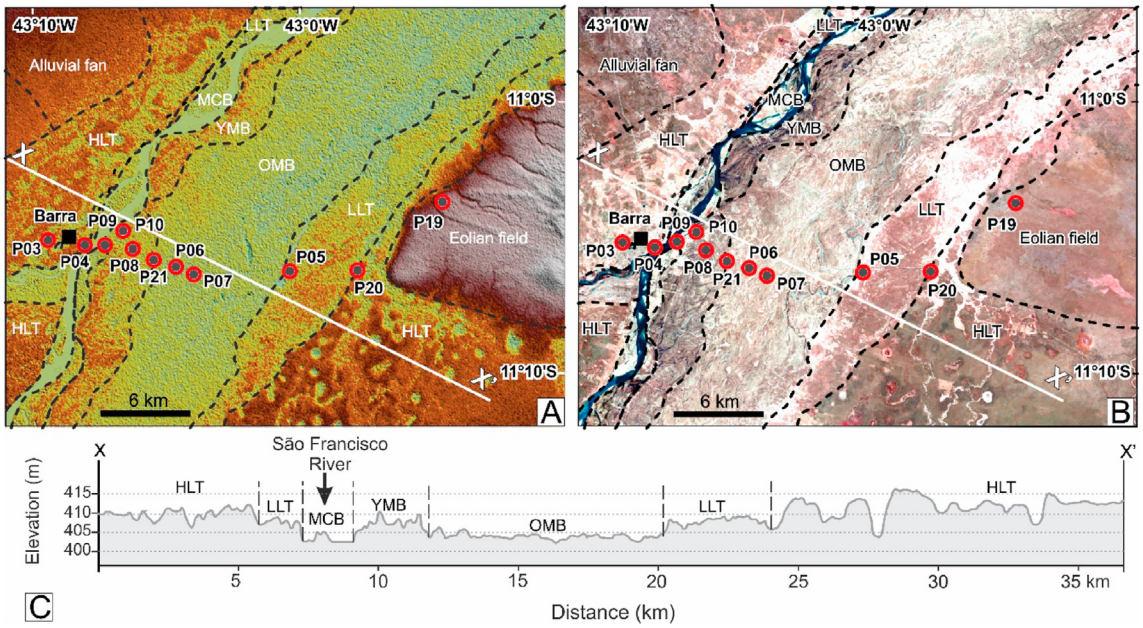

Fig. 5. Geomorphological compartmentation and altimetric section. A) SRTM digital elevation model (30 m); B) LANDSAT 8 OLI image, false color composition RGB (743); C) Altimetric section, with interpretation of the geomorphological compartments. Abbreviations: HLT (high-level terrace), LLT (low-level terrace), OMB (old meander belt), YMB (young meander belt), MCB (modern channel belt). (For interpretation of the references to color in this figure legend, the reader is referred to the Web version of this article.)

medium to coarse-grained sands with cross-stratification and fine sands with climbing ripples, forming fining-upward sequences, interspersed with layers of silty-clayey sediments (Fig. 9). Pedogenesis is limited, characterized by the presence of Fluvisols, bioturbation, and Fe and Mn mottling, mainly in clay deposits. Three OSL ages, from 0.4 ± 0.1 to 0.3 ± 0.1 ka (Table 1) indicate deposition during the 17th century AD, but the age of onset of sedimentation of the MCB could not be established because the dated sample was recovered from the upper part of the deposits in this zone.

4.2.6. Eolian dune field

The eolian dune field (EDF) is a morphological zone dominated by sand sheets, which form an extensive area on the west bank of the river plain and a smaller one on its east bank (Fig. 3). Dunes of varying dimensions, most of them stabilized by Caatinga vegetation, with predominant migration direction towards WNW, are the main depositional features (Fig. 10). Parabolic megadunes stand out in the landscape, either as simple dunes (elongate; *sensu* Pye, 1993) or as compound dunes (nested, digitate, and superimposed; *sensu* Pye, 1993), with heights up to 30 m in the nose, trailing arm length varying between 1.2 and 16.3 km and widths ranging from 0.9 to 5.6 km, with average transport direction azimuth of 292°. Smaller compound parabolic dunes, with en-echelon and lobate morphologies, arm length of 0.3–2.0 km and width of 0.3–0.6 km, and predominant migration direction towards azimuth 301° occur extensively in the area, covering even parts of the parabolic

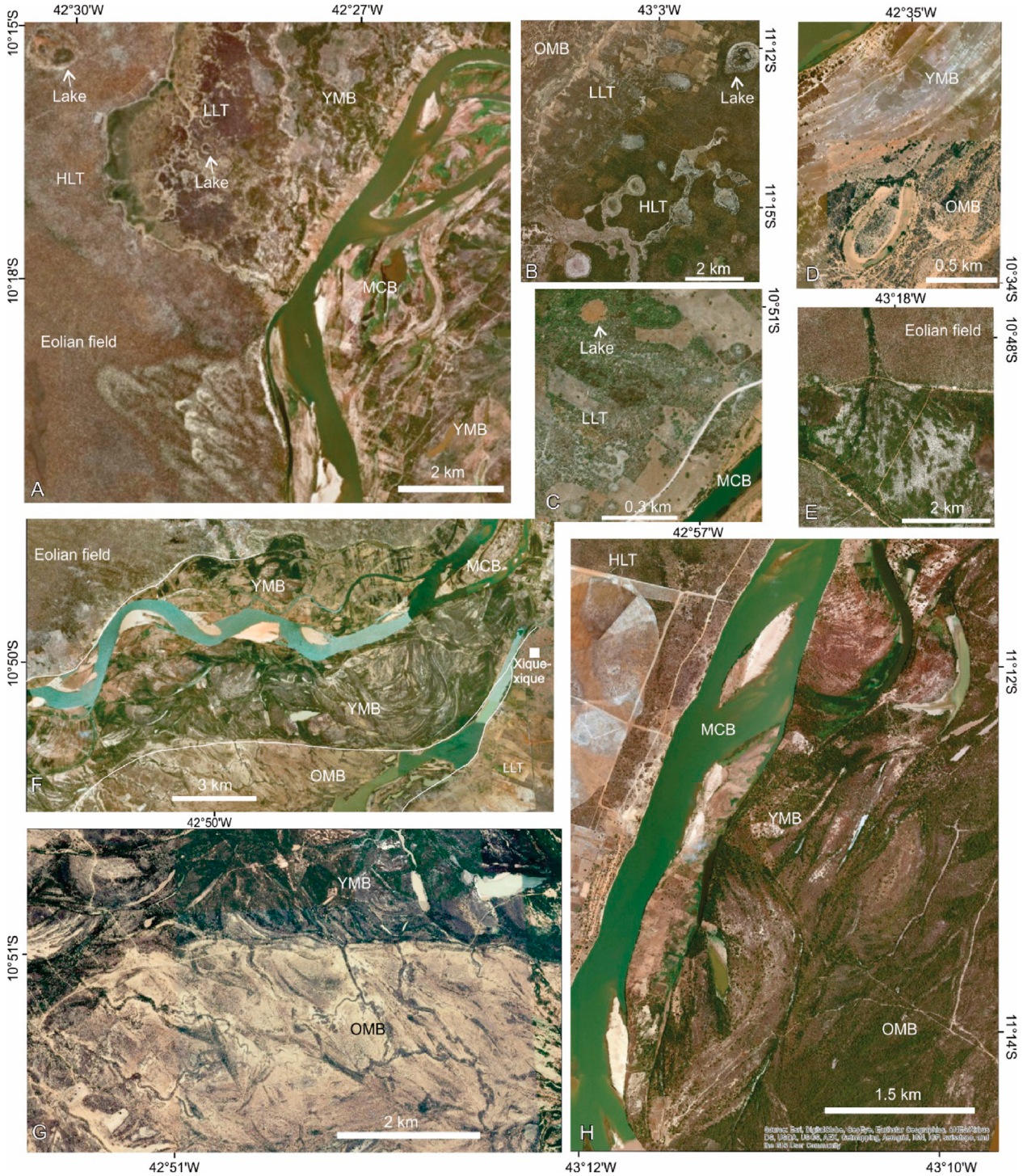

Fig. 6. Geomorphological features of the area. A) Morphologic relationships between the eolian dune field, HLT (lake highlighted), LLT (smaller lake), YMB and MCB; B) Highlight of the HLT, with coalescing lakes; C) LLT, with lake smaller than the one on HLT; D) Abandoned meander in the OMB; E) Alluvial fan reworking the eolian deposits; F and G) Cutting feature of the YMB onto OMB; H) Modern meander belt with low sinuosity over the YMB, with preserved meander scrolls; Abbreviations: HLT (high-level terrace), LLT (low-level terrace), OMB (old meander belt), YMB (young meander belt), MCB (modern channel belt). Aerial images extracted from the World Imagery plugin of ArcGIS online.

megadunes. Some dunes show signs of recent reactivation, especially in the vicinity of the left river bank where there are recent small coalescent parabolic dunes, with a height of up to 20 m and short arms, with only a few tens of meters.

Deposits are composed of well-sorted fine/medium-grained quartz sands, with few grains of heavy minerals and feldspar, and unconsolidated. In some shallow trenches it was possible to recognize cross-stratification and concentrations of millimeter-sized charcoal fragments 2 m below the surface. The eolian deposits form sand sheets mainly over the surface of the HLT, but they can also occur onto pedogenized deposits of the LLT (e.g., in P01; Fig. 7).

The oldest ages of the eolian deposits were obtained from OSL dating (Table 1) on sands of a parabolic megadune (P19) and from

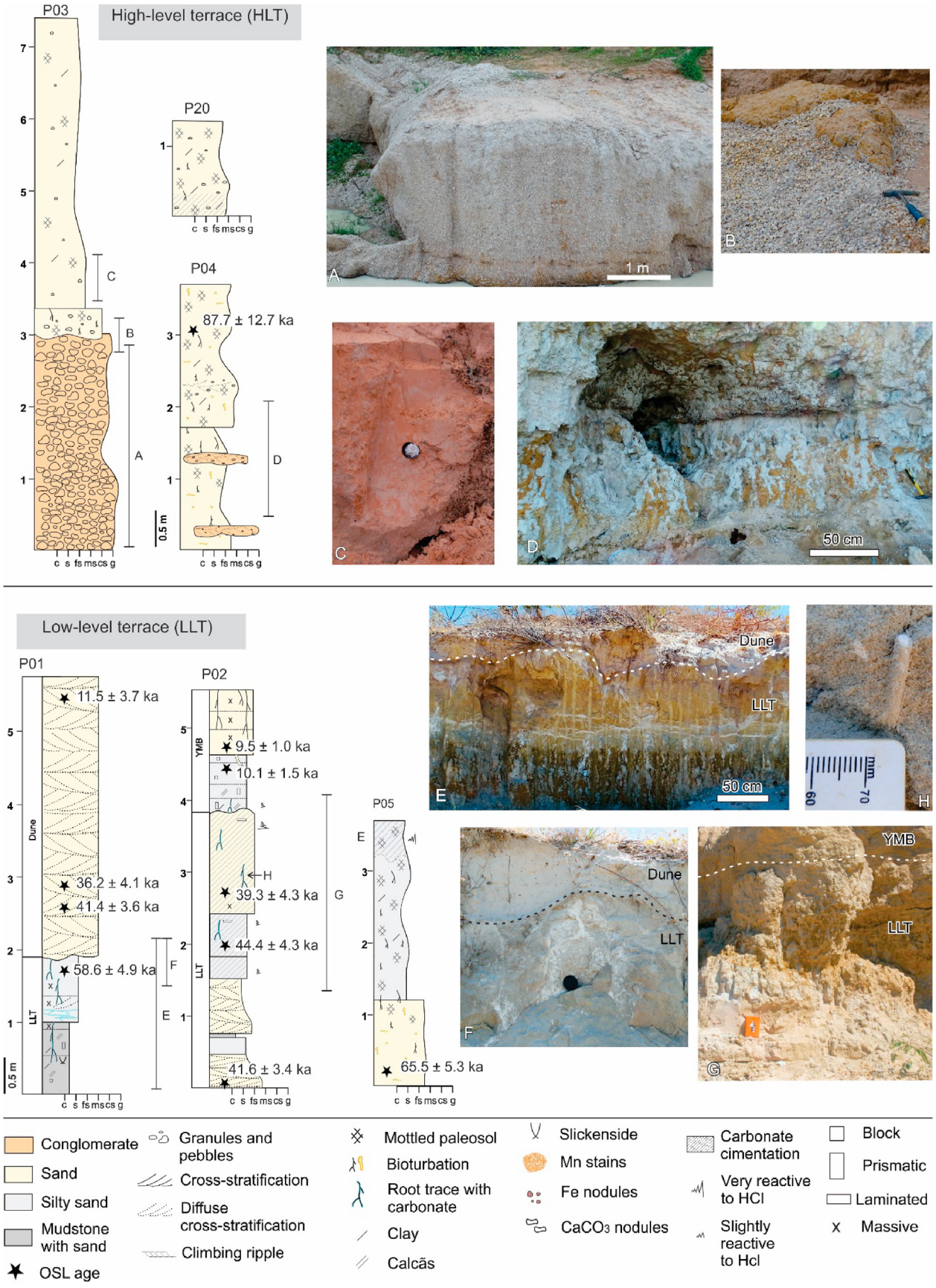

Fig. 7. Sedimentary vertical profiles and pictures of degradational surfaces deposits.

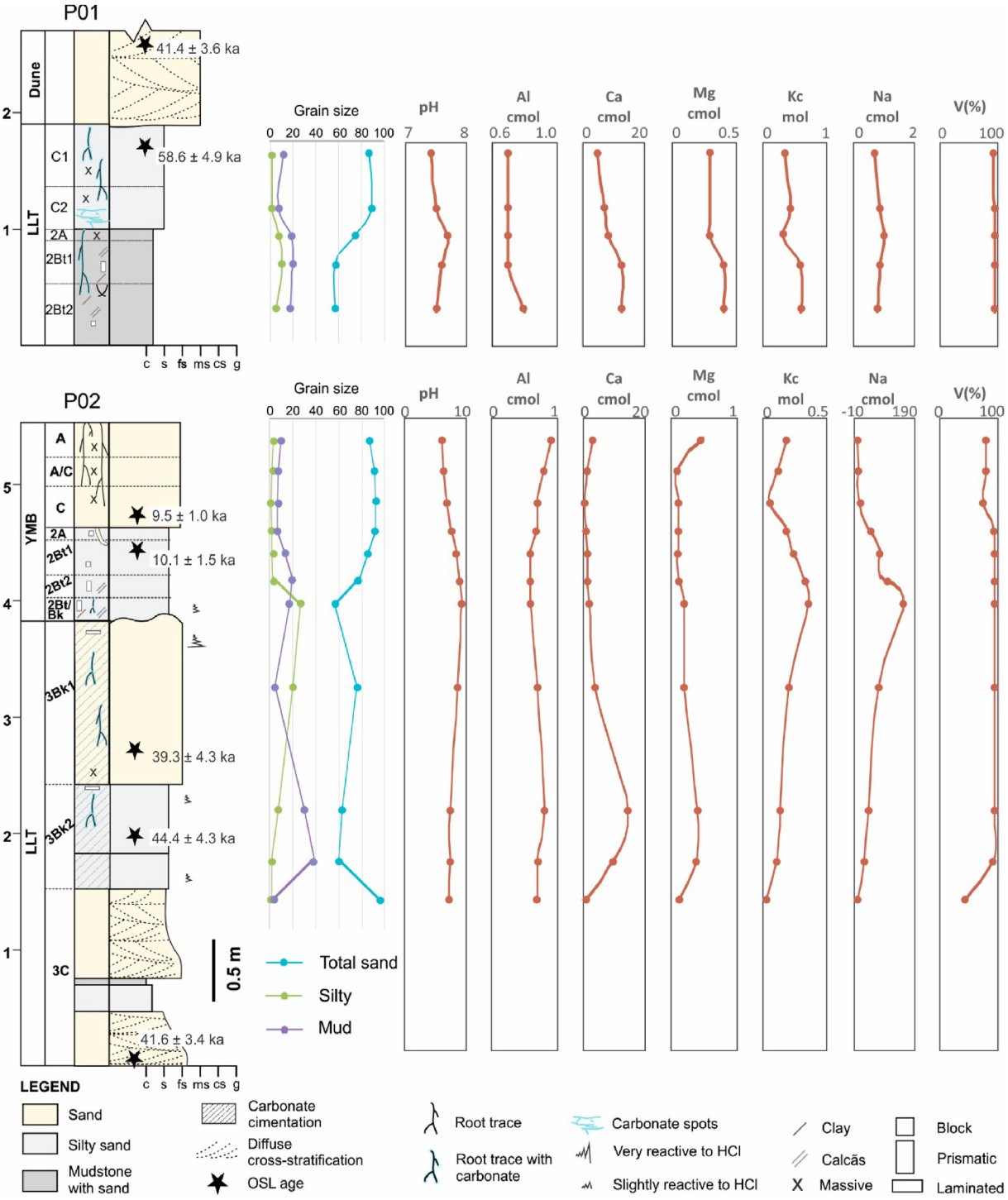

Fig. 8. Low-level terrace sedimentary vertical profiles, with pedologic detailing (horizons and pedogenic features), grain size and chemistry.

eolian deposits exposed on the left-margins of the São Francisco River (P01), revealing that the dune field was active during the Late Pleistocene (45.1 ± 5.2 to 25.5 ± 4.4 ka). The other five ages, from samples of sand recovered in trenches dug at the top of the dunes (<1.5 m depth), yielded ages between 14.3 ± 2.6 and 5.2 ± 1.4 ka, showing strong wind activity with migration of parabolic dunes during the Early/Middle Holocene and stabilization after 5 ka.

5. Interpreting the sequence of aggradation and incision events

The differences in elevation, contact relationships, and ages of the deposits of the mapped geomorphological zones allowed to establish the succession of events that originated the current configuration of the middle São Francisco river plain (Fig. 11). The

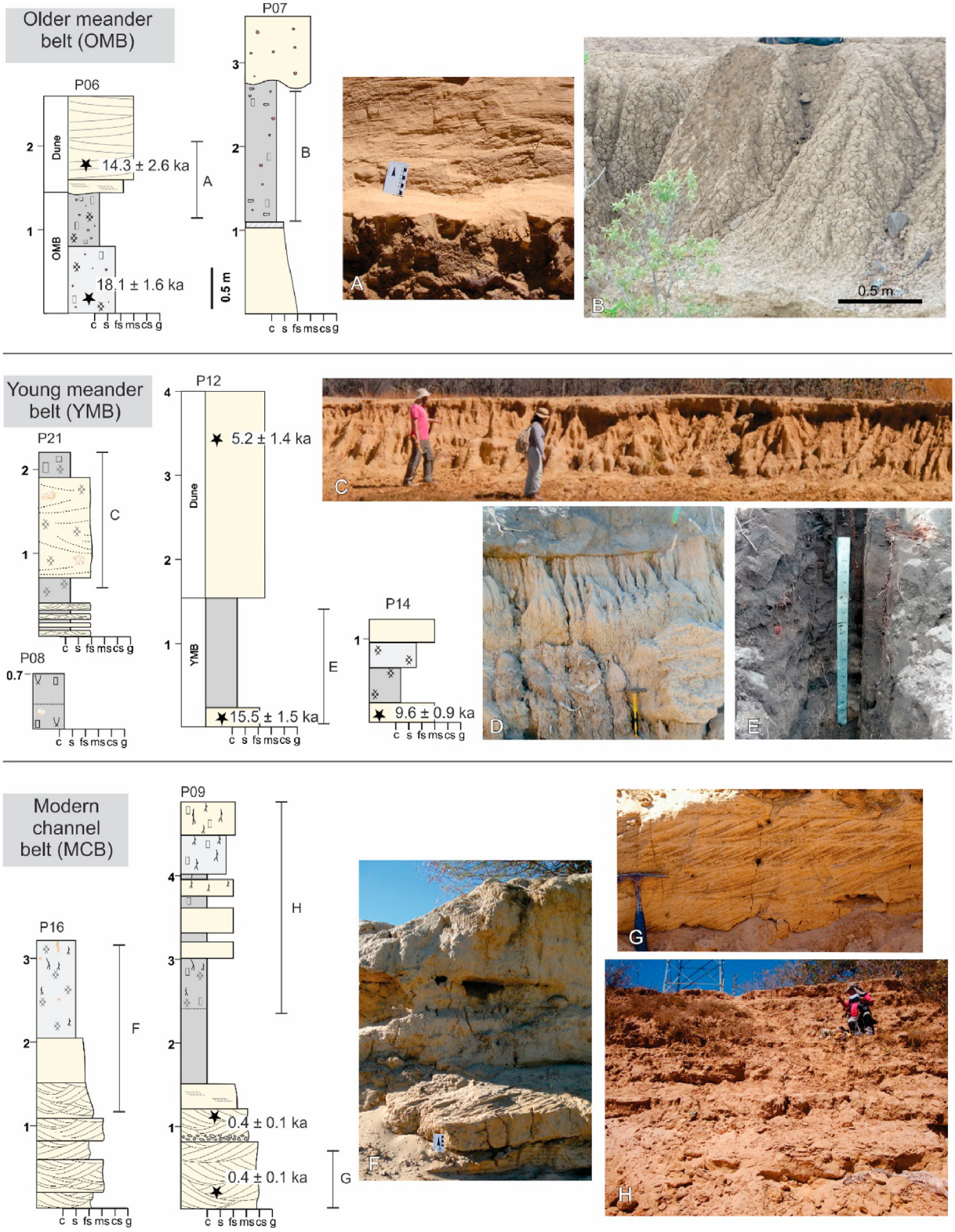

Fig. 9. Sedimentary vertical profiles and pictures of the aggradational fluvial deposits. (Legend of the profiles is the same as in Fig. 7).

deposits that make up the HLT are the oldest; the only available age indicates active sedimentation during the MIS 5 (87.7 ± 12.7 ka), but sedimentation started much earlier because the sample dated was recovered from the upper part of the terrace. As the surface of the HLT is degraded, without original morphological elements preserved and punctuated by numerous lakes formed after the deposition, the depositional paleoenvironment reconstruction presents many uncertainties.

Based on the fact that the HLT occurs throughout the lowland of the middle course of the São Francisco River, extending to the base

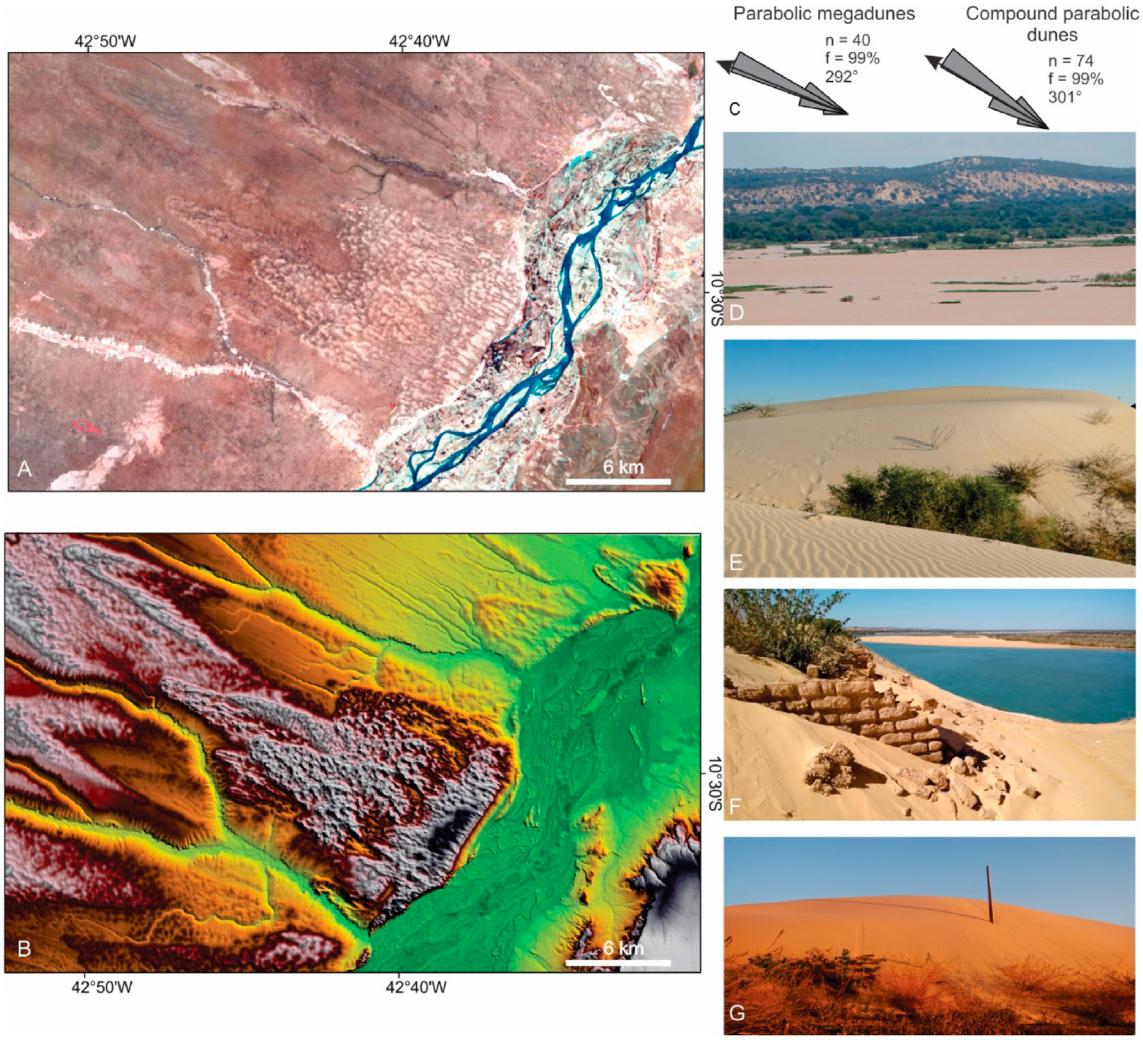

Fig. 10. Dunes of the eolian field. A) LANDSAT 8 OLI image, false color composition RGB (743); B) Digital elevation model provided by the Brazilian army; C) Transport direction azimuth (n = number of measurements, f = consistency factor); D) Stabilized dunes in the margin of the São Francisco River; E) Parabolic morphology of the active dunes in the area; F) Ruins of a building being covered by active dunes; G) Transmission line pole partially covered by active dunes. (For interpretation of the references to color in this figure legend, the reader is referred to the Web version of this article.)

of the rocky reliefs of the surrounding highlands, the most plausible interpretation is that its sedimentation occurred in an unconfined alluvial plain, formed by the coalescence of a trunk river and tributary rivers from the highlands, with no genetic relationship with the modern river plain (Fig. 11). The existence of outcrops with up to 3-m-thick layers of clast-supported conglomerates interspersed with sands, and the rarity of fine-grained facies, allows interpretation of past braided rivers, with a different depositional tract compared to the later fluvial plains. With the aggradation of the alluvial plain, the deposits underwent generalized pedogenesis, with development of thick profiles with several paleosol horizons. Soils with hydromorphic characteristics indicate that the plain was subject to frequent flooding.

The first incision (I1), constrained by ages between 87.7 ± 12.7 ka and 65.5 ± 5.3 ka, created an entrenched plain on the previous deposits and records the regional lowering of the erosion base level. Since the valley was wide, as there are terraces in the HLT hillslope on both sides of the São Francisco plain, the incision was also marked by significant lateral erosion caused by migration of the channel during formation of the entrenched plain.

The LLT has no preserved depositional shapes and their deposits of fine-grained facies, often fining upwards, allows tentatively to interpret deposition in a meandering fluvial system. Deposits with ages between 65.5 ± 5.3 and 39.3 ± 4.3 ka currently preserved in the LLT record a long period of aggradation in an entrenched fluvial plain, from the middle MIS 4 to the middle MIS 3. This aggradational period is also recorded in the upper river course, as indicated by deposits of river terraces in the tributary Das Velhas River (Magalhães Jr. et al., 2011; Fig. 12).

The LLT deposits, like those of the HLT, were affected by carbonate pedogenesis, but an important feature differentiates the imprint of this pedogenesis in the sedimentary deposits of the two terraces. Well-developed paleosol carbonates, with carbonate rhizoconcretions, occur close to the surface in the LLT deposits. Differently, carbonate levels are less expressive and occur a few meters below the surface in the HLT deposits, indicating that the water table during the pedogenesis was shallow in the LLT and deeper in the HLT. The lakes, characteristic of the degradational plains, occur over siliciclastic deposits intensively cemented by carbonates. The formation mechanism of these lakes is hypothetically associated with the dissolution of the carbonate cement from the deposits and soils of these terraces, observed in several exposures.

The second incision event (I2) is younger than 39.3 ± 4.3 ka,

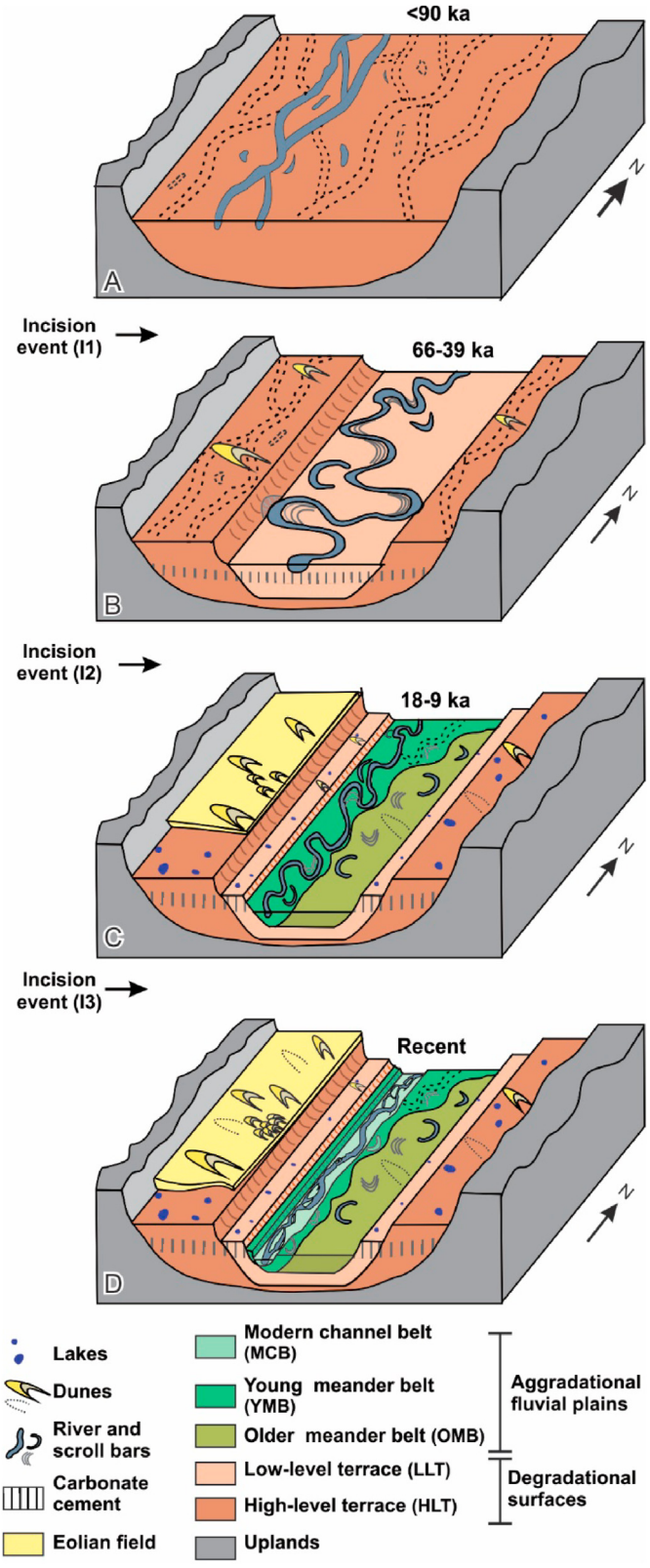

Fig. 11. Schematic model of the geomorphological and sedimentary evolution of the medium course of the São Francisco River during the late Quaternary.

occurring after the formation of the carbonate paleosols. It gave rise to meander belts in the aggradational plain where the current river channel is located. The incision is older than 18.1 ± 1.6 ka, obtained from the only available OSL age of OMB scroll bar deposits; it was not possible to establish the start of the fall of the regional erosion base level. Concomitantly to channel deepening by vertical incision (stream downcutting), the river widened the valley by lateral erosion, forming deposits of scroll bars in a meandering river. Fluvial incision corresponding to I2 is also recorded in the upstream tributary Das Velhas River (Magalhães Jr. et al., 2011).

The OMB has small, incised channels on its surface forming incipient tributary drainage truncated by the YMB scrolls bars (Fig. 6), which indicate a lowering event of the channel before the formation of the younger belt. However, aggradation is evident in the southern part of the area during the formation of the YMB, where its scrolls truncate and are topographically higher than the OMB scrolls, showing this sedimentation was continuous from the terminal Pleistocene to the Early Holocene (18.1 ± 1.6 to 9.5 ± 1.0 ka). Correlated narrow terraces were recognized on the banks of the Icatu River, a tributary on the left bank of the São Francisco, with a similar age (15.5 ± 1.5 ka). Correlatable deposits upstream, in the Das Velhas River (Magalhães Jr. et al., 2011), suggest that aggradation extended to the Middle Holocene.

OSL ages younger than 9.5 ± 1.0 ka were absent in sediments of the meander belts. This absence suggests that the river remained in equilibrium with sediment bypass in the Middle/Late Holocene, possibly functioning as source of a great part of the sands that formed eolian dunes on its left bank (14.3 ± 2.6 to 5.2 ± 1.4 ka).

The MCB is narrow and incised, and the river has lateral and central sandy bars, displaying a new channel pattern completely different from the meander belts. Sinuosity index is extremely low (1.1), and the channel is twice wider than the channels of the abandoned meander belts. The sedimentary facies are also different, with sands coarser than those of the abandoned meander belts (OMB and YMB) and the lower terrace (LLT). The lowering of the base level in the São Francisco River caused riverbed degradation in the Icatu River. As the Icatu valley cuts eolian deposits of 7.6 ± 0.7 to 5.2 ± 1.4 ka, the São Francisco hydraulic regime changed during the Late Holocene. The São Francisco River is overfit and resulted from riverbed degradation, which implies the existence of a Late Holocene incision event (I3). The MCB deposits dated are young (0.4 ka), not allowing to define when the present channel pattern was established.

6. Fluvial response to quaternary climate changes

Paleoclimatic interpretations based on fluvial deposits should be made with great caution in extensive watersheds, especially in tectonically quiescent areas in the interior of continents controlled by local base levels. Events of fluvial incision can result from thalweg lowering (riverbed degradation) due to hydrological changes, frequently related to enhanced river discharge, and decreasing vegetation cover (Tucker and Slingerland, 1997). To understand fluvial aggradation/incision events in the semi-arid São Francisco River basin it is necessary to compare them with published local and regional paleoclimatic proxy data based on speleothems and palynomorphs. Our results, published proxy data, and Quaternary climate cycles are summarized in Fig. 12. Approximate intervals of aggradation and incision phases discussed in this section are derived from the OSL ages presented in Table 1.

This comparison has revealed itself difficult because the middle course of the São Francisco River is in a transitional zone, between the Southeast and Northeast regions of Brazil, which were paleoclimatically out of phase in some periods (Wang et al., 2006; Cruz et al., 2009; Cheng et al., 2013). The middle course of the São

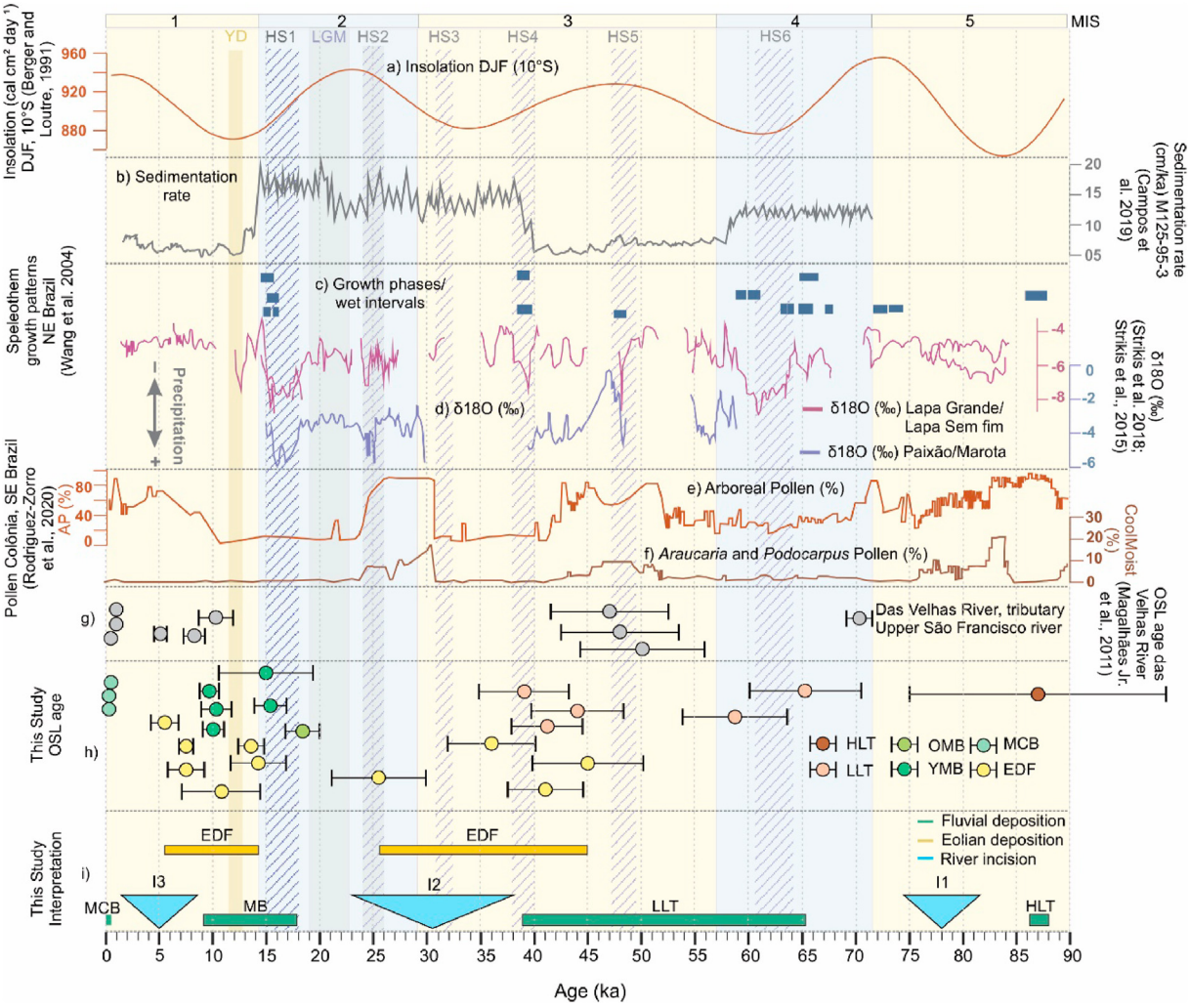

Fig. 12. Global cycles and regional proxies correlated with events of aggradation and incision in the São Francisco River. A) Insolation curve at 10°S for December to February (Berger and Loutre, 1991); B) Sedimentation rate of the São Francisco River in the marine core M125-95-3 (Campos et al., 2019); C) Growth phases of speleothems and calcareous tufa in northeast Brazil (Wang et al., 2004); D) $\delta^{18}O$ speleothem records from central-east (Lapa Grande and Lapa Sem Fim caves) and northeast (Paixão and Marota caves) Brazil (Strikis et al., 2015 e 2018); E) Arboreal pollen percentages (AP) from Colônia (CO3 and CO14; Rodríguez-Zorro et al., 2020); F) Percentage curve of the sum of cool moist conifers *Araucaria* and *Podocarpus* from Colônia (Rodríguez-Zorro et al., 2020); G) OSL dating of the Das Velhas River, tributary of the São Francisco River in its upper course (Magalhães Jr. et al., 2011); H) OSL dating in eolian and fluvial sediments of the middle course of the São Francisco River (this study); I) Interpretation of sedimentation and incision events of the middle course of the São Francisco River (age of HLT deposits is based on a single dating) (this study). Blue and yellow bars indicate the MIS – Marine Isotope Stage (Lisiecki and Raymon, 2005). Last Glacial Maximum – LGM, Heinrich Stadials – HS; and Younger Dryas – YD, according to Mix et al. (2001), Sanches Goñi and Harrison (2010) and Rasmussen et al. (2014) respectively. (For interpretation of the references to color in this figure legend, the reader is referred to the Web version of this article.)

Francisco is considered to be in phase with the Northeast Brazil during the Last Glacial Maximum (LGM), but in antiphase during the Lower/Middle Holocene (Cruz et al., 2009; Strikis et al., 2018).

Late Pleistocene (MIS 5) deposits of the HLT record the oldest sedimentary aggradation event in the lowland areas within the drainage basin area and have no genetic relationship with the modern fluvial plain. The age from this unit (88 ka) shows deposition contemporaneous to a wet period recorded by a speleothem growth phase in northeastern Brazil (Wang et al., 2004).

Paleoprecipitation data from nearby cave speleothems reveal a dominantly dry period with short wet intervals during the first event of fluvial incision (I1, 85 to 66 ka) (Wang et al., 2004; Strikis et al., 2015, 2018). During the middle MIS 4 to the middle MIS 3 (66 to 39 ka) the São Francisco River showed a long period of aggradation registered in the LLT deposits, also recorded in deposits of terraces in the upper course of the river (Magalhães Jr. et al., 2011; Fig. 12). Discontinuous speleothem data show dominantly dry conditions with short wet periods, the latter associated with Heinrich events (Wang et al., 2004; Strikis et al., 2015, 2018). Water table fluctuations in a dominantly dry alluvial environment are interpreted based on the carbonate pedogenesis (Kelson et al., 2020), that affects deposits of both terraces and is eolian active approximately between 45 and 25 ka.

The second incision event (I2) took place between 39 and 18 ka, during the transition from MIS 3 to MIS 2, also recorded upstream (Magalhães Jr. et al., 2011). During this time interval, paleoprecipitation curves show dominantly dry conditions with short wet periods, particularly during HS4 and HS2 (Strikis et al., 2015, 2018). The beginning of the I2 event (HS4) is correlated with more humid moments, marked by phases of speleothem growth (Wang et al., 2004).

Eolian field dunes developed during periods of predominant drier local climates and increased sediment availability, deposited in the river valley during previous aggradational phases. Eolian sand deposition occurred mainly during the second half of the MIS 3, starting at the twilight of LLT aggradational phase (45 ka).

Geochemical data from marine sediments offshore Northeast Brazil indicate drier conditions during the MIS 3, with humidity peaks coinciding with Heinrich events (Arz et al., 1998, 1999, 1999; Behling et al., 2000; Mulitza et al., 2017; Campos et al., 2019; Mendes et al., 2019). Eolian processes and dune migration remained active during I2 until 26 ka, favored by low precipitation and sediment supply derived mainly from the river plain. Local humid climate from 26 to 15 ka, encompassing the HS1 and HS2 high precipitation events (Wang et al., 2004; Strikis et al., 2018), had an important role in dune stabilization, with development of vegetation cover.

Following a period of relatively drier conditions during the LGM (Cruz et al., 2009; Mulitza et al., 2017; Strikis et al., 2018; Mendes et al., 2019), the HS1 was the most significant humid event in the middle São Francisco basin (Wang et al., 2004; Strikis et al., 2018), which possibly functioned as a corridor for south-derived montane forest taxa to reach northern areas (Pinaya et al., 2019). The two meander belts (OMB and YMB) started to be formed after the LGM (18 to 9 ka). Paleoprecipitation proxy data from speleothems and palynomorphs indicate that aggradation began under very humid local conditions during HS1 but continued under prevailing drier conditions in the Early Holocene (Oliveira et al., 1999; Strikis et al., 2018). This climate change to more arid conditions enhanced the effectiveness of wind processes and enabled dune reactivation during the Early/Middle Holocene. Like today, trade winds were dominant, causing dune migration towards WNW (Figs. 10 and 13).

The modern river channel is overfit and resulted from riverbed degradation. However, this event of increased fluvial discharge that resulted in the incision event (I3) is not related to augmented local rainfall because the Late Holocene was a period of aridity in the middle São Francisco River basin (Oliveira et al., 1999; Strikis et al., 2018).

This sequence of events shows that periods of increased fluvial discharge necessary to climate-driven incisions have no correlation with local climate because paleoprecipitation data from nearby cave speleothems show dominant dry periods with short wet intervals during the events of incision. Alternatively, changes in fluvial discharge can be controlled by climate changes in the upper catchment zone. Humid climates and increased fluvial discharge in the upper course cause lowering of riverbed over long distances downstream (Knighton, 1998) and the adjustment to a more concave profile (Zaprowski, 2005). Incision is more effective if accompanied by sediment yield reduction, caused by changes to vegetation that protects the soil and reduce hillslope erosion. Following initial riverbed degradation and thalweg lowering, lateral erosion due to channel migration can cause valley widening. Inversely, the return to aggradational conditions results from reduction in fluvial discharge or increase in sedimentary supply, or a combination of both factors.

The north-flowing São Francisco River crosses different climatic zones latitudinally controlled, today from the semi-humid headwaters (17-20° S) to the semi-arid lower course (10-11° S). Nearly 65% of the fluvial discharge in the middle/lower course is derived from the catchment area in the upper course (Fig. 1), which is in the pathway of the South Atlantic Convergence Zone (SACZ; Fig. 13), that migrates north-south mediated by insolation/precession cycles (Bernal et al., 2016). The three recognized events of fluvial incision fit well with cycles of solar radiation energy, coinciding with the moment of radiation rises (Fig. 12). Since insolation/precession cycles influence variations in the activity of the SACZ, we hypothesize they are a main control of events of fluvial incision and enhanced fluvial discharge.

An important location to comprehend the role of SACZ here is the Campestre lake of Salitre (19° S, elevation 970 m), located in the São Francisco upper course (Ledru, 1993; Ledru et al., 1996). The

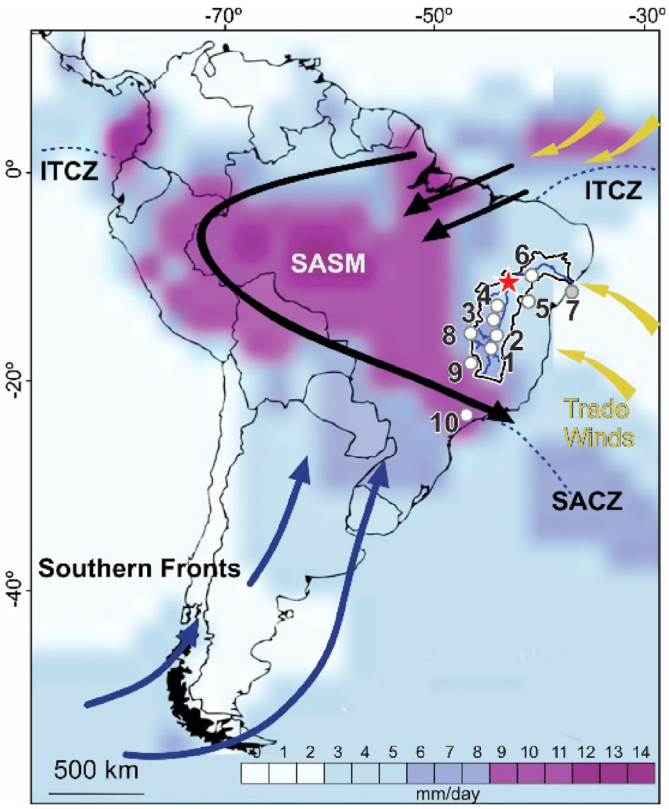

Fig. 13. Map of South America, showing the distribution of precipitation, plotted as the long-term mean annual precipitation from 1981 to 2010 using data from the Global Precipitation Climatology Project (GPCP) (modified from Rodríguez-Zorro et al., 2020). South American summer monsoon (SASM; black arrows), and the position of the Intertropical and South Atlantic convergence zones (ITCZ and SACZ; blue dashed lines) during the austral summer in South America (DJF) are represented as well. Blue arrows show the northernmost position of the year-round southern fronts. Yellow arrows indicate prevailing wind direction. The black polygon refers to the São Francisco River basin and numbers refer to the regional datasets to be compared with this study (red star); 1. Das Velhas River (Magalhães Jr. et al., 2011); 2–3. Lapa Sem Fim, and Lapa Grande caves (Strikis et al., 2015, 2018); 4. Padre cave (Wang et al., 2007); 5. Paixão and Marota caves (Strikis et al., 2015, 2018); 6. Caves and travertine deposits of northeastern Brazil (Wang et al., 2004); 7. Core M125-9503 (Campos et al., 2019); 8. Lagoa Feia (Cassino et al., 2020); 9. Lagoa Campestre in Salitre (Ledru et al., 1996); 10. Colônia (Rodríguez-Zorro et al., 2020). (For interpretation of the references to color in this figure legend, the reader is referred to the Web version of this article.)

interval ~50–40 ka was arid in that site, but northward shifts of polar fronts changed local climate and the vegetation adapted to a cold period of high moisture from 40 to 30 ka, with the development of floodplain forests from 33 to 28 ka (Ledru et al., 1996), that probably persisted until 23 ka (Ledru, 1993). This humid period, characterized by the expansion of forests in the source-area, coincides with fluvial incision (I2) triggered by enhanced fluvial discharge in the middle course. New data show global climate shifts ca. 42 ka caused by the combination of geomagnetic field minima and Grand Solar Minima (Adams Event; Cooper et al., 2021). These shifts may have been the global trigger for this more humid period recorded by palynological (Ledru, 1993; Ledru et al., 1996) and speleothem (Strikis et al., 2015, 2018) proxies in the middle of MIS3, and the change from aggradation to incision recorded in the São Francisco River. The proportion of arboreal pollens declined from 17 to 10 ka in the Salitre site, an unstable period characterized by rapid climatic and vegetational changes there (Ledru, 1993), when meander belts formed in the middle course of the São Francisco River. During the Holocene, the climate became warm and humid (after 9 ka), with expansion of Araucaria and semi-deciduous

forests at the Salitre site, coinciding with the ending of meander belts evolution and the Holocene incision (I3) in the middle course of the São Francisco River.

There is little paleoclimate information along the SACZ to corroborate our hypothesis, but good correlation exists between incision events and humid periods recorded at the Colonia site (23°52' S), characterized by high percentages of Araucaria, Podocarpus, and arboreal pollen (Rodriguez-Zorro, 2020, Fig. 12). These humid events along the SACZ seem to have controlled the upper course of the Paraná River, located south of the São Francisco drainage, where an incision event (27–12 ka) partially contemporaneous to I2 was recorded (Oliveira et al., 2019).

From source to sink, sediments eroded during incision events were transported downstream and deposited in strandplain/deltaic systems or eventually in submarine settings. Data from piston core collected from the continental slope (1897 m water depth, Campos et al., 2019, Fig. 12) show a partial correlation between the high sedimentation rate in the river mouth and incision events in the middle São Francisco (Fig. 12). The beginning of the second incision event (I2) is exceptionally well correlated with an increase in the sedimentation rate recorded in the core (Fig. 12; Campos et al., 2019). However, the highest sedimentation rate from 21 to 14 ka seems to have no correspondence with incision events in the middle São Francisco; instead, it correlates with incision in the exposed continental shelf during a period of low sea level associated with LGM. During the last incision event (I3), the sedimentation rate is low in the core, probably because sediment was trapped in coastal strandplain systems and eolian dune fields (Dominguez, 1996; Barbosa and Dominguez, 2004). These indicate that sedimentation rates in submarine settings near river mouths show a clear correlation, but do not reflect only paleoprecipitation in the interior drainage basin, particularly in long plateau rivers controlled by interior base levels.

7. Conclusions

The OSL dating method was used for the first time in the sedimentary deposits of the middle São Francisco River. This allowed the creation of a robust chronological framework to constrain the succession of alluvial aggradational and degradational phases and the interplay between alluvial and eolian sedimentation in the last 100 ka. We identified seven geomorphological zones in the area: (1) High-level terrace (87.7 ± 12.7 ka); (2) Low-level terrace (65.5 ± 5.3 to 39.3 ± 4.3 ka); (3) Older meander belt (18.1 ± 1.6 ka); (4) Young meander belt (15.5 ± 1.5 to 9.5 ± 1.0 ka); (5) Modern channel belt (0.4 ± 0.1 to 0.3 ± 0.1 ka); (6) Eolian dune fields (45.1 ± 5.2 to 25.5 ± 4.4 ka and 14.3 ± 2.6 to 5.2 ± 1.4 ka); (7) Active alluvial fans. Zones 1 and 2 are older degraded surfaces, forming terraces made up of older alluvial deposits. Zones 3 to 5 constitute the modern confined aggradational plain. Eolian dune fields of zone 6 occupy an extensive area on the left-margins of the river.

Before ca. 88 ka, the São Francisco River had higher flow rates and likely a braided pattern. From ca. 66 ka, it evolved into a meandering pattern, and finally reached the current braided/straight morphology during the Late Holocene (<1 ka). The widespread carbonate pedogenic cementation over the terraces indicates a drier climate phase in the region, probably around the end of the MIS 3 (~37 ka). Carbonate cement dissolution is likely the mechanism responsible for the generation of depressions hosting lakes on the degraded surfaces.

We recognized three phases of fluvial incision (I1 − 85 to 66 ka; I2 − 39 to 18 ka and I3 − 9 to 1.0 ka), and two phases of dune field stabilization (25–15 ka and 5 ka to recent). Development of the eolian dune field occurred during periods of predominant local drier conditions that allowed reworking of the fluvial plain by inland activity of trade winds. The aggradation events (66–39 ka and 18 to 9 ka) and the incision event (I2) are also observed in the upper course of the São Francisco River.

We hypothesize that the events of fluvial incision were triggered by increased fluvial discharge in the upper catchment area, resulted from variations in the activity of the SACZ, controlled by precession cycles. The events of high sedimentation rate in the São Francisco river mouth are partially correlated with incision phases in its middle course. This suggests that sedimentation can be decoupled across the drainage basin, especially in plateau rivers with interior base levels and large extensions.

Author statement

Herewith we return to you the revised version of our manuscript entitled "*Fluvial aggradation and incision in the Brazilian tropical semi-arid: climate-controlled landscape evolution of the São Francisco River*". All authors improved the manuscript through corrections and suggestions. Patricia C. Mescolotti: conceptualization, formal analysis, investigation, writing - original draft and visualization. Fabiano N. Pupim: investigation, methodology and writing - Original Draft; Francisco B. Ladeira: methodology, formal analysis and investigation; André O. Sawakuchi: methodology and resources; Amanda S. Catharina: writing - original draft and visualization; Mario Assine: conceptualization, writing - original draft, project administration, funding acquisition.

Acknowledgments

The authors thank José Cândido Stevaux, Gisele Utida and Vinícius Ribau Mendes for fieldwork assistance; Universidade Federal do Oeste da Bahia, Campus of Barra, for logistical support, and Thays Minelli and Luciana Nogueira for laboratory support. AOS (#304727/2017–2), FBL (#307951/2018–9), FNP (#302411/2018–6) and MLA (#304925/2017–9) are research fellows of Brazilian National Council for Scientific and Technological Development - CNPq/Brazil. PCM is grateful for the scholarship from CNPq. This work was supported by the FAPESP, Brazil, through PIRE NSF-FAPESP (2017/50085–3).

Appendix A. Supplementary data

Supplementary data to this article can be found online at https://doi.org/10.1016/j.quascirev.2021.106977.

References

Ab'Sáber, A., 2006. O paleodeserto de Xique-Xique. Estud. Avançados 20, 301–308.
Aitken, M.J., 1985. Thermoluminescence Dating. Academic Press, London.
Alvares, C.A., Stape, J.L., Sentelhas, P.C., de Moraes, G., Leonardo, J., Sparovek, G., 2013. Köppen's climate classification map for Brazil. Meteorol. Z. 22, 711–728.
Arnold, L.J., Roberts, R.G., 2009. Stochastic modeling of multi-grain equivalent dose (De) distributions: implications for OSL dating of sediment mixtures. Quat. Res. 55, 159–167.
Arz, H.W., Pätzold, J., Wefer, G., 1998. Correlated millennial-scale changes in surface hydrography and terrigenous sediment yield inferred from last-glacial marine deposits off northeastern Brazil. Quat. Res. 50, 157–166.
Arz, H.W., Pätzold, J., Wefer, G., 1999. Climatic changes during the last deglaciation recorded in sediment cores from the northeastern Brazilian Continental Margin. Geo Mar. Lett. 19, 209–218.
Aufdenkampe, A.K., Mayorga, E., Raymond, P.A., Melack, J.M., Doney, S.C., Alin, S.R., Aalto, R.E., Yoo, K., 2011. Riverine coupling of biogeochemical cycles between land, oceans, and atmosphere. Front. Ecol. Environ. 9 (11), 53–60.
Barbosa, L.M., Dominguez, J.M.L., 2004. Coastal dune fields at the São Francisco River strandplain, northeastern Brazil: morphology and environmental controls. Earth Surf. Process. Landforms 29, 443–456.
Barreto, A.M.F., Suguio, K., Oliveira, P.E. de, Tatumi, S.H., 2002. Campo de dunas inativas do médio Rio São Francisco, BA: marcante registro de ambiente desértico do quaternário brasileiro. Sitios geológicos e paleontológicos do Bras.
Behling, H., Arz, H.W., Pätzold, J., Wefer, G., 2000. Late Quaternary vegetational and

climate dynamics in northeastern Brazil, inferences from marine core GeoB 3104-1. Quat. Sci. Rev. 19, 981–994.
Berger, A., Loutre, M.-F., 1991. Insolation values for the climate of the last 10 million years. Quat. Sci. Rev. 10, 297–317.
Bernal, J.P., Cruz, F.W., Stríkis, N.M., Wang, X., Deininger, M., Catunda, M.C.A., Auler, A.S., 2016. High-resolution Holocene south American monsoon history recorded by a speleothem from botuverá cave, Brazil. Earth Planet Sci. Lett. 450, 186–196.
Camargo, O.A., Moniz, A.C., Jorge, J.A., Valadares, J., 2009. Métodos de Análise Química, Mineralógica e Física de Solos do Instituto Agronômico de Campinas.
Campos, M.C., Chiessi, C.M., Prange, M., Mulitza, S., Kuhnert, H., Paul, A., Venancio, I.M., Albuquerque, A.L.S., Cruz, F.W., Bahr, A., 2019. A new mechanism for millennial scale positive precipitation anomalies over tropical South America. Quat. Sci. Rev. 225, 105990.
Cassino, R.F., Ledru, M.-P., de Almeida Santos, R., Favier, C., 2020. Vegetation and fire variability in the central Cerrados (Brazil) during the Pleistocene-Holocene transition was influenced by oscillations in the SASM boundary belt. Quat. Sci. Rev. 232, 106209.
Chaves, R.R., Cavalcanti, I.F.A., 2001. Atmospheric circulation features associated with rainfall variability over southern Northeast Brazil. Mon. Weather Rev. 129, 2614–2626.
Cheng, H., Sinha, A., Cruz, F.W., Wang, X., Edwards, R.L., d'Horta, F.M., Ribas, C.C., Vuille, M., Stott, L.D., Auler, A.S., 2013. Climate change patterns in Amazonia and biodiversity. Nat. Commun. 4, 1–6.
Cooper, A., Turney, C.S.M., Palmer, J., Hogg, A., McGlone, M., Wilmshurst, J., et al., 2021. A global environmental crisis 42,000 years ago. Science 371 (6531), 811–818.
Cruz, F.W., Vuille, M., Burns, S.J., Wang, X., Cheng, H., Werner, M., Edwards, R.L., Karmann, I., Auler, A.S., Nguyen, H., 2009. Orbitally driven east–west anti-phasing of South American precipitation. Nat. Geosci. 2, 210–214.
Dominguez, J.M.L., 1996. The São Francisco strandplain: a paradigm for wave-dominated deltas? Geol. Soc. London, Spec. Publ. 117, 217–231. https://doi.org/10.1144/GSL.SP.1996.117.01.13.
Dominguez, J.M.L., Bittencourt, A.C.S.P., Martin, L., 1983. O papel da deriva litorânea de sedimentos arenosos na construção das planícies costeiras associadas às desembocaduras dos rios São Francisco (SE-AL), Jequitinhonha (BA), Doce (ES) e Paraíba do Sul (RJ). Rev. Bras. Geociencias 13, 98–105.
Galbraith, R.F., Roberts, R.G., Laslett, G.M., Yoshida, H., Olley, J.M., 1999. Optical dating of single and multiple grains of quartz from Jinmium rock shelter, northern Australia: Part I, experimental design and statistical models. Archaeometry 41, 339–364.
Guérin, G., Mercier, N., Adamiec, G., 2011. Dose-rate conversion factors: update. Anc. TL 29, 5–8.
Kelson, J.R., Huntington, K.W., Breecker, D.O., Burgener, L.K., Gallagher, T.M., Hoke, G.D., Petersen, S.V., 2020. A proxy for all seasons? A synthesis of clumped isotope data from Holocene soil carbonates. Quat. Sci. Rev. 234, 106259.
Knighton, D., 1998. Fluvial Forms and Processes, Fluvial Forms and Processes: A New Perspective. Routledge. https://doi.org/10.4324/9780203784662.
Knoppers, B., Medeiros, Paulo, R.P., Souza, Weber, F.L., Jennerjahn, T., 2006. The Sao Francisco Estuary, Brazil, in: Estuaries. Springer Science & Business Media, p. 51.
Latrubesse, E.M., Stevaux, J.C., Sinha, R., 2005. Tropical rivers. Geomorphology 70, 187–206.
Ledru, M.-P., 1993. Late Quaternary Environmental and Climatic Changes in Central Brazil. Quat. Res. YORK LONDON-ACADEMIC Press. vol. 39, 90.
Ledru, M.-P., Braga, P.I.S., Soubiès, F., Fournier, M., Martin, L., Suguio, K., Turcq, B., 1996. The last 50,000 years in the Neotropics (Southern Brazil): evolution of vegetation and climate. Palaeogeogr. Palaeoclimatol. Palaeoecol. 123, 239–257.
Lisiecki, L.E., Raymo, M.E., 2005. A Pliocene-Pleistocene stack of 57 globally distributed benthic δ18O records. Paleoceanography 20.
Magalhães Junior, A.P., Cherem, L.F.S., de Paula Barros, L.F., dos Santos, G.B., 2011. OSL dating of sediments from a mountainous river in southeastern Brazil: late Cenozoic tectonic and climatic implications. Geomorphology 132, 187–194.
P.C. Mendes, V.R., Sawakuchi, A.O., Chiessi, M., Giannini, C.F., Rehfeld, K., Mulitza, S., 2019. Thermoluminescence and optically stimulated luminescence measured in marine sediments indicate precipitation changes over northeastern Brazil Paleoceanogr. Paleoclimatology 34, 1476–1486.
Merino, E.R., do Nascimento Pupim, F., de Azevedo Macedo, H., Assine, M.L., 2015. Realce e integração de imagens orbitais óticas com dados SRTM para mapeamento e estudo de grandes planícies fluviais: exemplos de aplicação no Pantanal. Rev. Bras. Geomorfol. 16.
Mix, A.C., Bard, E., Schneider, R., 2001. Environmental processes of the ice age: land, oceans, glaciers (EPILOG). Quat. Sci. Rev. 20, 627–657.
Mulitza, S., Chiessi, C.M., Schefuß, E., Lippold, J., Wichmann, D., Antz, B., Mackensen, A., Paul, A., Prange, M., Rehfeld, K., 2017. Synchronous and proportional deglacial changes in Atlantic meridional overturning and northeast Brazilian precipitation. Paleoceanography 32, 622–633.
Murray, A.S., Wintle, A.G., 2003. The single aliquot regenerative dose protocol: potential for improvements in reliability. Radiat. Meas. 37, 377–381.
Murray, A.S., Wintle, A.G., 2000. Luminescence dating of quartz using an improved single-aliquot regenerative-dose protocol. Radiat. Meas. 32, 57–73.
Nazareno, A.G., Dick, C.W., Lohmann, L.G., 2019. A biogeographic barrier test reveals a strong genetic structure for canopy-emergent Amazon tree species. Sci. Rep. 9, 18602.
Oliveira, P.E., Barreto, A.M.F., Suguio, K., 1999. Late Pleistocene/Holocene climatic and vegetational history of the Brazilian caatinga: the fossil dunes of the middle São Francisco River. Palaeogeogr. Palaeoclimatol. Palaeoecol. 152, 319–337.
Oliveira, S.C., Pupim, F.N., Stevaux, J.C., Assine, M.L., 2019. Luminescence chronology of terrace development in the Upper Paraná River, southeast Brazil. Front. Earth Sci. 7, 200.
Pereira, S.B., Pruski, F.F., Silva, D.D. da, Ramos, M.M., 2007. Estudo do comportamento hidrológico do Rio São Francisco e seus principais afluentes. Rev. Bras. Eng. Agrícola Ambient. 11, 615–622.
Pinaya, J.L.D., Cruz, F.W., Ceccantini, G.C.T., Corrêa, P.L.P., Pitman, N., Vemado, F., Maria del Carmen, S.L., Pereira Filho, A.J., Grohmann, C.H., Chiessi, C.M., 2019. Brazilian montane rainforest expansion induced by Heinrich Stadial 1 event. Sci. Rep. 9, 1–14.
Prescott, J.R., Hutton, J.T., 1994. Cosmic ray contributions to dose rates for luminescence and ESR dating: large depths and long-term time variations. Radiat. Meas. 23, 497–500.
Pye, K., 1993. Late Quaternary development of coastal parabolic megadune complexes in northeastern Australia, in: Aeolian Sediments. Ancient and Modern. Blackwell Scientific Publications, pp. 23–44.
Rasmussen, S.O., Bigler, M., Blockley, S.P., Blunier, T., Buchardt, S.L., Clausen, H.B., Cvijanovic, I., Dahl-Jensen, D., Johnsen, S.J., Fischer, H., 2014. A stratigraphic framework for abrupt climatic changes during the Last Glacial period based on three synchronized Greenland ice-core records: refining and extending the INTIMATE event stratigraphy. Quat. Sci. Rev. 106, 14–28.
Retallack, G.J., 2001. Soils of the Past. Oxford, Blackwell, 404p.
Rodríguez-Zorro, P.A., Ledru, M.-P., Bard, E., Aquino-Alfonso, O., Camejo, A., Daniau, A.-L., Favier, C., Garcia, M., Mineli, T.D., Rostek, F., 2020. Shut down of the South American summer monsoon during the penultimate glacial. Sci. Rep. 10, 1–11.
Sanchez Goñi, M.F., Harrison, S.P., 2010. Millennial-scale climate variability and vegetation changes during the Last Glacial: concepts and terminology. Quat. Sci. Rev. 29, 2823–2827.
Santos, A.Á.B., Camargo, O., Back, A., Silva, F., Catani, F., Estante, F., Lima, G., Violato, G., Araújo, J., Andrade, P., 2013. Atlas Eólico Bahia.
Santos, H. de A., dos Santos, P.P., Kenji, D.O.L., 2012. Changes in the flood regime of São Francisco river (Brazil) from 1940 to 2006. Reg. Environ. Change 12, 123–132.
Schoeneberger, P.J., Wysocki, D.A., Benham, E.C., 2012. Field Book for Describing and Sampling Soils. Government Printing Office.
Singh, A., Thomsen, K.J., Sinha, R., Buylaert, J.-P., Carter, A., Mark, D.F., Mason, P.J., Densmore, A.L., Murray, A.S., Jain, M., Paul, D., Gupta, S., 2017. Counter-intuitive influence of Himalayan river morphodynamics on Indus Civilisation urban settlements. Nat. Commun. 8, 1617.
Smedley, R.K., Duller, G.A.T., Rufer, D., Utley, J.E.P., 2020. Empirical assessment of beta dose heterogeneity in sediments: implications for luminescence dating. Quat. Geochronol. 56, 101052.
Stríkis, N.M., Chiessi, C.M., Cruz, F.W., Vuille, M., Cheng, H., de Souza Barreto, E.A., Mollenhauer, G., Kasten, S., Karmann, I., Edwards, R.L., 2015. Timing and structure of mega-SACZ events during Heinrich stadial 1. Geophys. Res. Lett. 42, 5477–5484A.
Stríkis, N.M., Cruz, F.W., Barreto, E.A.S., Naughton, F., Vuille, M., Cheng, H., Voelker, A.H.L., Zhang, H., Karmann, I., Edwards, R.L., 2018. South American monsoon response to iceberg discharge in the North Atlantic. Proc. Natl. Acad. Sci. Unit. States Am. 115, 3788–3793.
Tamura, T., Nguyen, V.L., Ta, T.K.O., Bateman, M.D., Gugliotta, M., Anthony, E.J., Nakashima, R., Saito, Y., 2020. Long-term sediment decline causes ongoing shrinkage of the Mekong megadelta. Vietnam. Scientific Reports 10, 8085.
Thom, G., Xue, A.T., Sawakuchi, A.O., Ribas, C.C., Hickerson, M.J., Aleixo, A., Miaky, C., 2020. Quaternary climate changes as speciation drivers in the Amazon floodplains. Science Advances 6, eaax4718.
Tucker, G.E., Slingerland, R., 1997. Drainage basin responses to climate change. Water Resour. Res. 33, 2031–2047. https://doi.org/10.1029/97WR00409.
Wang, X., Auler, A.S., Edwards, R.L., Cheng, H., Cristalli, P.S., Smart, P.L., Richards, D.A., Shen, C.-C., 2004. Wet periods in northeastern Brazil over the past 210 kyr linked to distant climate anomalies. Nature 432, 740–743.
Wang, X., Auler, A.S., Edwards, R.L., Cheng, H., Ito, E., Solheid, M., 2006. Interhemispheric anti-phasing of rainfall during the last glacial period. Quat. Sci. Rev. 25, 3391–3403.
Wang, X., Auler, A.S., Edwards, R.L., Cheng, H., Ito, E., Wang, Y., Kong, X., Solheid, M., 2007. Millennial-scale precipitation changes in southern Brazil over the past 90,000 years. Geophys. Res. Lett. 34.
Zaprowski, B.J., 2005. Climatic influences on profile concavity and river incision. J. Geophys. Res. 110, F03004. https://doi.org/10.1029/2004JF000138.